

SHORT COMMUNICATION



Design, synthesis, and *in vitro* evaluation of aza-peptide aldehydes and ketones as novel and selective protease inhibitors

Thomas S. Corrigan^a, Leilani M. Lotti Diaz^a, Sarah E. Border^a, Steven C. Ratigan^b, Kayla Q. Kasper^a, Daniel Sojka^c, Pavla Fajtova^d, Conor R. Caffrey^d, Guy S. Salvesen^e, Craig A. McElroy^b, Christopher M. Hadad^a and Özlem Doğan Ekici^{a,f}

^aDepartment of Chemistry and Biochemistry, The Ohio State University, Columbus, OH, USA; ^bDivision of Medicinal Chemistry and Pharmacognosy, College of Pharmacy, The Ohio State University, Columbus, OH, USA; ^cInstitute of Parasitology, Biology Centre of the Czech Academy of Sciences, Ceske Budejovice, Czech Republic; ^dCenter for Discovery and Innovation in Parasitic Diseases, Skaggs School of Pharmacy and Pharmaceutical Sciences, University of California San Diego, La Jolla, CA, USA; ^eSanford Burnham Prebys Medical Discovery Institute, La Jolla, CA, USA; ^fDepartment of Chemistry and Biochemistry, The Ohio State University at Newark, Newark, OH, USA

ABSTRACT

Aza-peptide aldehydes and ketones are a new class of reversible protease inhibitors that are specific for the proteasome and clan CD cysteine proteases. We designed and synthesised aza-Leu derivatives that were specific for the chymotrypsin-like active site of the proteasome, aza-Asp derivatives that were effective inhibitors of caspases-3 and -6, and aza-Asn derivatives that inhibited *S. mansoni* and *I. ricinus* legumains. The crystal structure of caspase-3 in complex with our caspase-specific aza-peptide methyl ketone inhibitor with an aza-Asp residue at P1 revealed a covalent linkage between the inhibitor carbonyl carbon and the active site cysteinyl sulphur. Aza-peptide aldehydes and ketones showed no cross-reactivity towards cathepsin B or chymotrypsin. The initial *in vitro* selectivity of these inhibitors makes them suitable candidates for further development into therapeutic agents to potentially treat multiple myeloma, neurodegenerative diseases, and parasitic infections.

ARTICLE HISTORY

Received 13 February 2020
Accepted 8 May 2020

KEYWORDS

Proteasome inhibitor; caspase and legumain inhibitors; aza-peptide carbonyls; anticancer; antiparasitic

Introduction



Aza-peptides are peptidomimetics where the α -carbon centre of one or more of the natural amino acids in a peptide chain is replaced with a nitrogen atom (Figure 1). This modification results in the loss of chirality of the amino acid and a bend in the peptide chain. Previously, it has been shown that the aza-substitution in biologically active peptide analogs has led to enhanced metabolic stability and selectivity for the biological targets¹. Hence, in medicinal chemistry, aza-peptides have been employed in many roles including enzyme inhibitors, activity-based probes, ligands for receptors, imaging agents, pro-drugs, and drugs. While studies on retro hydrazino-aza-peptoids have been attempted with the proteasome before², aza-peptide aldehydes and ketones emerge as a new class of electrophilic protease inhibitors for multiple proteases. Here we report the design, synthesis, and kinetic evaluation of aza-peptide aldehydes and ketones that are specific for the proteasome, caspases, and legumain.


Incorporation of the aza-peptide motif in protease inhibition was first introduced by Dolle and co-workers³. Several aza-peptidyl inhibitors, including aza-peptide halomethyl ketones and aza-peptide ketones, were designed and synthesised to target the clan CA cysteine proteases cathepsin B and calpain, as well as the serine proteases chymotrypsin and elastase. All of them were found to be ineffective inhibitors of these enzymes. However, to date, several

other classes of aza-peptidyl inhibitors have been reported as potent and selective inhibitors of other proteases. Aza-peptide epoxides and aza-peptide Michael acceptors have been shown to potently and selectively inhibit clan CD proteases such as caspases, legumains, gingipains, and clostripain by Powers and co-workers^{4–7}. Aza-peptide nitriles were developed as effective and stable inhibitors for clan CA proteases such as cathepsins L, S, and K by Guetschow^{8,9}.

In our design, the α -carbon of the P1 amino acid is replaced with a nitrogen, making it an aza-P₁ residue (Figure 1). A carbonyl group is attached to the P₁ aza-amino acid replacing the scissile bond of the natural substrate and creating the novel aza-peptide aldehyde or ketone warhead.

The proteasome is a threonine protease and plays a central role in the ubiquitin-mediated degradation of unwanted proteins in the cell¹⁰. The proteasome is 750 kDa in molecular mass and has three active sites within its 20S catalytic core: chymotrypsin-like (CT-L), trypsin-like (T-L), and caspase-like (C-L)¹¹. Inhibition of the proteasome, which has been shown to be overexpressed in tumour cells¹², leads to cellular apoptosis of the affected cells. Therefore, this inhibition strategy has been validated as an effective treatment for multiple myeloma patients¹³. Inhibitors, such as the aza-peptide aldehydes and ketones described here, are designed to cease proteolysis of mis-folded and unwanted proteins through the selective inhibition of the CT-L active site. Development of the proteasome inhibitor blockbuster drugs bortezomib (FDA-approved in 2003),

CONTACT Özlem Doğan Ekici  dogan-ekici.1@osu.edu  Department of Chemistry and Biochemistry, The Ohio State University at Newark, Newark, OH 43055, USA

 Supplemental data for this article can be accessed [here](#).

© 2020 The Author(s). Published by Informa UK Limited, trading as Taylor & Francis Group.

This is an Open Access article distributed under the terms of the Creative Commons Attribution License (<http://creativecommons.org/licenses/by/4.0/>), which permits unrestricted use, distribution, and reproduction in any medium, provided the original work is properly cited.

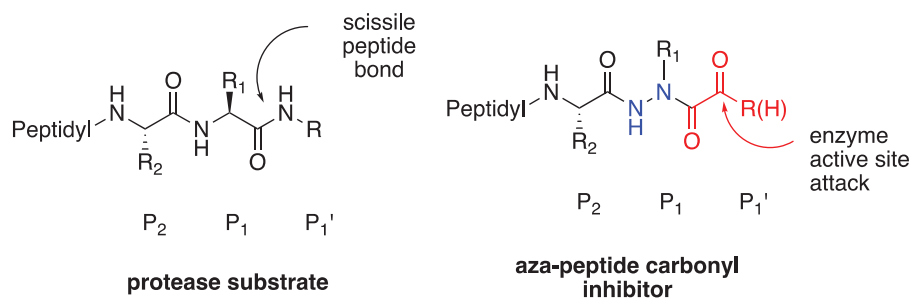


Figure 1. Aza-peptide aldehyde and ketone design.

carfilzomib^{14,15} (FDA-approved in 2012) and ixazomib (FDA-approved in 2015) revolutionised the treatment of multiple myeloma, significantly prolonging the lives of patients¹⁶. However, bortezomib shows severe side effects, such as peripheral neuropathy, in up to 64% of newly diagnosed multiple myeloma patients,^{17,18} largely due to off-target inhibition, by bortezomib's boronic acid warhead¹⁹, of HtrA2/Omi, a serine protease involved in neuronal survival. Carfilzomib has been shown to result in less peripheral neuropathy, but lately it has been associated with adverse cardiovascular effects in up to 30% of the treated patients²⁰. Ixazomib is an oral formulation and also possesses a boronic acid warhead; thus, peripheral neuropathy is still a major side effect. Therefore, careful dosing or discontinuation is also essential with ixazomib, as drug-induced peripheral neuropathy can be irreversible²¹. Hence, the search for new proteasome inhibitors is an ongoing challenge.

Caspases are a family of cysteine proteases that belong to a small clan, the clan CD cysteine proteases. They have a strict requirement for peptides containing an Asp residue at the P₁ position for substrate cleavage; hence, the name caspase evolved from "cysteiny l aspartate specific protease." To date, there are 14 caspases identified in humans. Most importantly, caspases are the key-mediators of apoptosis (programmed cell death), and these enzymes play essential roles in inflammation and neurodegeneration^{22,23}. Hence, they have been recognised as novel therapeutic targets for central nervous system diseases in which cell death occurs mainly by an apoptotic mechanism²⁴. The roles of caspases in the mechanism of apoptosis has been studied extensively since the mid-1990s^{25,26}. Caspase-3 is a key executioner caspase responsible either partially or totally for proteolytic cleavage of key apoptotic proteins²⁷. It functions to decrease or destroy essential homeostatic pathways during the effector phase of apoptosis. Caspase-3 cleaves or activates nuclear enzymes, such as poly(ADP-ribose) polymerase (PARP), the 70 kDa subunit of the U1 small ribonucleoprotein, the catalytic subunit of DNA-dependent protein kinase, and protein kinase C δ ²⁸. Compared to the rest of the caspases, caspase-3 is found to be inherently high in abundance in biological environments. In addition, caspase-3 has higher absolute k_{cat}/K_m values in general⁵. Therefore, most caspase-specific inhibitors will show anti-apoptotic activity via inhibition of caspase-3, also due to high cross-reactivity among caspases themselves. A good caspase inhibitor has to possess a P₁ Asp as it is a strict requirement for the caspase family. It is with this motivation, we designed inhibitors specific for caspase-3 with the DEVD sequence. Lately, caspase-6 has been shown to cleave many proteins important in neurodegeneration such as tau, amyloid precursor protein and Huntingtin protein²⁹. Hence, an effective caspase-6 inhibitor may offer treatments for neurodegenerative diseases, including Alzheimer's Disease and Huntington's Disease.

Legumains are also clan CD cysteine proteases, sharing a common fold with caspases that is unique to this clan. Legumains are acidic lysosomal enzymes that strictly require an asparagine residue

at the P₁ position in order to cleave substrate peptides³⁰. Legumain is abundant in human solid tumours and promotes cell migration, tissue invasion and metastasis³¹. The overexpression of legumain in tumour tissues³² makes it an attractive target for cancer therapy. Legumain has been described in plants; mammals^{33,34}; the human blood fluke, *Schistosoma mansoni*³⁵; the protozoan parasite, *Trichomonas vaginalis*⁷; and the ticks, *Ixodes ricinus*³⁶ and *Haemaphysalis longicornis*³¹. In the intestine of *S. mansoni* and *I. ricinus*, legumains contribute to digestion of the blood meal proteins³⁷, including haemoglobin, and *trans*-activate other protease zymogens involved in protein digestion³⁸. Therefore, in addition to cancer therapy, the selective inhibition of legumains also offers a therapeutic opportunity to effectively treat the diseases caused or transmitted by these parasites³⁹ which affect over 200 million people worldwide, with a great majority being located in Africa⁴⁰.

Herein, we show that aza-peptide aldehydes and ketones are selective inhibitors with considerable activity against the proteasome, caspases-3 and -6, as well as the legumains derived from *S. Mansoni* and *I. ricinus*.

Materials and methods

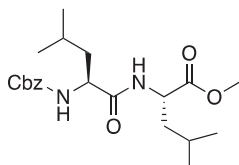
Chemistry

All described reactions were carried out in flame/oven-dried glassware under a nitrogen or argon atmosphere, unless otherwise noted. Starting chemical reagents were purchased from reputable suppliers (Sigma Aldrich, St. Louis, MO, USA; Fisher Scientific, Waltham, MA, USA; Matrix Scientific, Columbia, SC, USA; Acros Organics, Fair Lawn, NJ, USA) and used without further purification or purified in accordance with procedures described in *Purification of Common Laboratory Chemicals*. Product purification by flash chromatography was carried out using normal phase 40–64 μ m 60 Å silica gel from Sigma Aldrich or using a Teledyne Isco CombiFlash RF + UV auto column system. Dichloromethane, tetrahydrofuran, *N,N*-dimethylformamide, diethyl ether, and pentane solvents were obtained from a solvent purification system (with activated alumina columns). Triethylamine and diisopropylethylamine were freshly distilled over CaH₂ prior to use and stored under an argon atmosphere. NMR experiments were performed on Bruker 400, 700 or 850 MHz spectrometers. Chemical shifts are expressed in parts per million (δ , ppm) while coupling constant values (J) are given in Hertz (Hz). Residual solvent protons were used as internal standards: for ¹H NMR spectra CDCl₃ = 7.26 ppm, DMSO-d₆ = 2.50 ppm and D₂O = 4.79 ppm while for ¹³C NMR spectra CDCl₃ = 77.0 ppm and DMSO-d₆ = 41.23 ppm; CDCl₃ and DMSO-d₆ were purchased from Cambridge Isotope Laboratories. High resolution mass spectra were recorded on a Bruker MicroTOF II instrument with internal sodium formate calibrant under electrospray ionisation (ESI) conditions. Hydrogenations were carried out

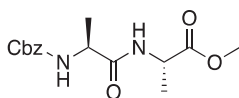
using a Parr hydrogenation apparatus. Kinetic assays were performed on a Molecular Devices SpectraMax i3.

Abbreviations. The following abbreviations have been used: AMC, 7-amino-4-methyl coumarin; AAla, aza-alanine residue; AAsp, aza-aspartic acid residue; AAsn, aza-asparagine residue; AGly, aza-glycine residue; ALeu, aza-leucine residue; Cbz, Ph-CH₂-OCO-; Pz, pyrazinyl; DCM, dichloromethane; DMF, *N,N*-dimethylformamide; DMSO, dimethyl sulfoxide; DTT, dithiothreitol; EtOAc, ethyl acetate; *i*BCF, isobutyl chloroformate; MeOH, methanol; NMM, *N*-methylmorpholine; NTA, nitrilotriacetic acid; RT, room temperature; TEV, tobacco etch virus; THF, tetrahydrofuran.

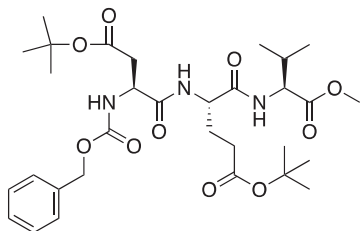
Peptide methyl esters



Methyl ((benzyloxy)carbonyl)-*L*-leucyl-*L*-leucinate (Cbz-Leu-Leu-OMe). Cbz-Leu-OH (5.3 g, 20 mmol) was dissolved in dry THF (200 ml) and cooled to -20°C . NMM (2.18 ml, 20 mmol) and *i*BCF (2.59 ml, 20 mmol) were added dropwise and the mixture was allowed to react for 30 min. Separately, H-Leu-OMe (3.6 g, 20 mmol) was dissolved in dry THF (200 ml) and cooled to -20°C and NMM (2.18 ml, 20 mmol) was added dropwise. This mixture was allowed to stir for 15 min. The two mixtures were then combined and allowed to stir for 1 h at -20°C . Following, the solution was allowed to stir while gradually warming to RT for 18 h. The solvent was removed *in vacuo*, and the resulting residue was dissolved with EtOAc, washed with 1 M HCl, H₂O, saturated NaHCO₃, and saturated brine. The organic layer was dried over Na₂SO₄, and concentrated *in vacuo* to afford the product as a white solid (7.0 g, 90% yield). ¹H NMR (DMSO-*d*₆, 400 MHz): 8.19 (d, *J* = 7.80 Hz, 1H), 7.39–7.28 (m, 5H), 5.00 (s, 2H), 4.33–4.25 (m, 1H), 4.12–4.01 (m, 1H), 3.59 (s, 3H), 1.71–1.36 (m, 6H), 0.93–0.81 (m, 12H).

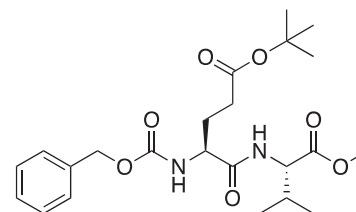


Methyl ((benzyloxy)carbonyl)-*L*-alanyl-*L*-alaninate (Cbz-Ala-Ala-OMe). See procedure and workup of Cbz-Leu-Leu-OMe. A white solid was obtained in 83% yield. ¹H NMR (DMSO-*d*₆, 400 MHz): 8.26 (d, *J* = 7.0 Hz, 1H), 7.40 (d, *J* = 7.6 Hz, 1H), 7.36 (m, 5H), 5.01 (d, *J* = 3.26 Hz, 2H), 4.27 (p, *J* = 7.16 Hz, 1H), 4.08 (p, *J* = 7.35 Hz, 1H), 3.62 (s, 3H), 1.29 (d, *J* = 7.3 Hz, 3H), 1.20 (d, *J* = 7.1 Hz, 3H).

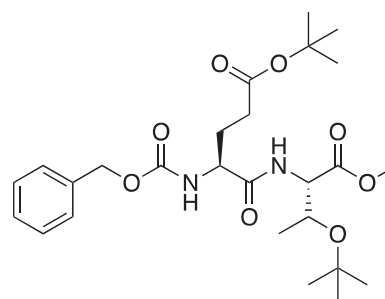


Methyl (5*S*,8*S*,11*S*)-5-(2-(*tert*-butoxy)-2-oxoethyl)-8-(3-(*tert*-butoxy)-3-oxopropyl)-11-isopropyl-3,6,9-trioxo-1-phenyl-2-oxa-4,7,10-triazadodecan-12-oate (Cbz-Asp(OtBu)-Glu(OtBu)-Val-OMe). See procedure and workup of Cbz-Leu-Leu-OMe. A white foam was obtained in 86% yield. ¹H NMR (DMSO-*d*₆, 400 MHz): 8.12 (d, *J* = 7.8 Hz, 1H),

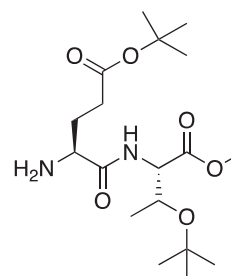
7.92 (d, *J* = 7.8 Hz, 1H), 7.60 (d, *J* = 8.3 Hz, 1H), 7.48–7.23 (m, 5H), 5.04 (d, *J* = 5.7 Hz, 2H), 4.42–4.30 (m, 1H), 4.00–4.19 (m, 2H), 3.62 (s, 3H), 2.65 (dd, *J* = 15.75, 5.66 Hz, 1H), 2.43 (dd, *J* = 16.1, 9.1 Hz, 1H), 2.22 (m, 2H), 2.04 (s, 1H), 1.94–1.81 (m, 1H), 1.79–1.67 (m, 1H), 1.40 (s, 10H, Boc and Val CH), 1.37 (s, 9H), 0.88 (t, *J* = 7.4 Hz, 6H).



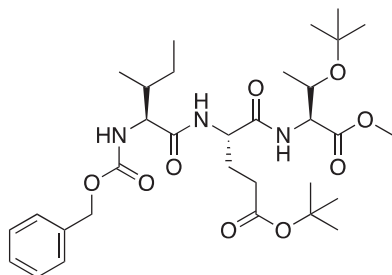
tert-Butyl (S)-4-(((benzyloxy)carbonyl)amino)-5-(((S)-1-methoxy-3-methyl-1-oxobutan-2-yl)amino)-5-oxopentanoate (Cbz-Glu(OtBu)-Val-OMe). See procedure and workup of Cbz-Leu-Leu-OMe. The product was obtained as a colourless oil in quantitative yield. ¹H NMR (DMSO-*d*₆, 400 MHz): 0.88 (t, 6H), 1.39 (s, 9H), 1.72 (m, 1H), 1.85 (m, 1H), 2.05 (q, 1H), 2.25 (t, 2H), 3.63 (s, 3H), 4.16 (m, 2H), 5.02 (d, 2H), 7.35 (m, 5H), 7.42 (d, 1H), 8.10 (d, 1H).



tert-Butyl (S)-4-(((benzyloxy)carbonyl)amino)-5-(((2*S*,3*S*)-3-(*tert*-butoxy)-1-methoxy-1-oxobutan-2-yl)amino)-5-oxopentanoate (Cbz-Glu(OtBu)-Thr(OtBu)-OMe). At -15°C a solution of Cbz-Glu(OtBu)-OH (6.74 g, 20 mmol) in THF (200 ml) was treated with NMM (2.97 ml, 20 mmol) and allowed to stir for 10 min. The solution was then treated with *i*BCF (2.59 ml, 20 mmol) and allowed to stir for 30 min at -15°C . A second solution of H-Thr(*t*Bu)-OMe (4.51 g, 20 mmol) in THF (200 ml) at -15°C was treated with NMM (2.97 ml, 20 mmol) and stirred for 15 min. The solutions were combined and stirred for 1 h at -15°C , then allowed to stir while gradually warming to RT for 16 h. The solvent was removed *in vacuo* and the resulting residue was dissolved in EtOAc, washed with 1 M HCl, H₂O, saturated Na₂HCO₃, and saturated brine. The organic layer was dried over Na₂SO₄ and removed *in vacuo* to afford the product as a white solid (8.07 g, 79% yield). ¹H NMR (DMSO-*d*₆, 400 MHz) δ : 7.67 (d, *J* = 8.8 Hz, 1H), 7.53 (d, *J* = 8.2 Hz, 1H), 7.41–7.27 (m, 5H), 5.03 (s, 2H), 4.35 (dd, *J* = 8.8, 2.7 Hz, 1H), 4.24–4.12 (m, 2H), 3.61 (s, 3H), 2.35–2.21 (m, 2H), 1.97–1.83 (m, 1H), 1.78–1.66 (m, 1H), 1.38 (s, 9H), 1.07 (s, 12H); HRMS (ESI) calcd for [C₂₆H₄₀N₂O₈+Na]⁺, 531.2685, found 531.2699 (M + 23).

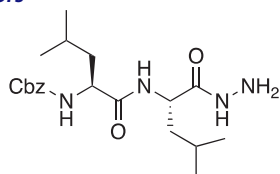


tert-Butyl (S)-4-amino-5-(((2S,3S)-3-(*tert*-butoxy)-1-methoxy-1-oxobutan-2-yl)amino)-5-oxopentanoate (H-Glu(OtBu)-Thr(OtBu)-OMe). A solution of *tert*-butyl (S)-4-(((benzyloxy)carbonyl)amino)-5-(((2S,3S)-3-(*tert*-butoxy)-1-methoxy-1-oxobutan-2-yl)amino)-5-oxopentanoate (8.07 g, 15.87 mmol) in MeOH (300 ml) was treated with 10% Pd/C and placed under H₂ at 40 psi for 2 h. The solution was filtered over Celite and concentrated *in vacuo* to afford the product as a white solid (5.36 g, 90% yield). ¹H NMR (DMSO-d₆, 400 MHz) δ: 8.03 (d, *J* = 9.1 Hz, 1H), 4.30 (dd, *J* = 9.0, 2.5 Hz, 1H), 4.16 (qd, *J* = 6.2, 2.6 Hz, 1H), 3.63 (s, 3H), 3.24 (dd, *J* = 7.9, 4.9 Hz, 1H), 3.17 (s, 1H), 2.30 (dd, *J* = 16.7, 8.5 Hz, 2H), 1.98–1.86 (m, 1H), 1.57 (dq, *J* = 13.7, 7.6 Hz, 1H), 1.39 (s, 9H), 1.08 (s, 12H); HRMS (ESI) calcd for [C₁₈H₃₄N₂O₆ + H]⁺, 375.2495, found: 375.2486 (M + 1).



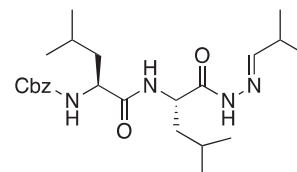
Methyl (5S,8S,11S)-8-(3-(*tert*-butoxy)-3-oxopropyl)-11-((S)-1-(*tert*-butoxy)ethyl)-5-((R)-*s*-butyl)-3,6,9-trioxo-1-phenyl-2-oxa-4,7,10-triazadodecan-12-oate *tert*-butyl (S)-4-(((benzyloxy)carbonyl)amino)-5-(((2S,3S)-3-(*tert*-butoxy)-1-methoxy-1-oxobutan-2-yl)amino)-5-oxopentanoate (Cbz-Ile-Glu(OtBu)-Thr(OtBu)-OMe). A solution of Cbz-Ile-OH (3.80 g, 14.33 mmol) in THF (100 ml) was cooled to –15 °C followed by the addition NMM (1.58 ml, 14.33 mmol) and allowed to stir for 10 min. The solution was then treated with iBCF (1.86 ml, 14.33 mmol) and allowed to stir for 30 min at –15 °C. Separately, a solution of *tert*-butyl (S)-4-amino-5-(((2S,3S)-3-(*tert*-butoxy)-1-methoxy-1-oxobutan-2-yl)amino)-5-oxopentanoate (5.37 g, 14.33 mmol) in THF (100 ml) at –15 °C was treated with NMM (1.58 ml, 14.33 mmol) and stirred for 15 min. The solutions were combined and allowed to stir for 1 h at –15 °C. Following, the solution was allowed to stir while gradually warming to RT for 16 h. The solvent was removed *in vacuo*, the resulting residue was dissolved in EtOAc, washed with 1 M HCl, H₂O, saturated Na₂HCO₃, and saturated brine. The organic layer was dried over Na₂SO₄ and concentrated *in vacuo* to afford the product as a white solid (6.30 g, 10.13 mmol, 70% yield). ¹H NMR (DMSO-d₆, 400 MHz) δ: 8.11 (d, *J* = 8.0 Hz, 1H), 7.68 (d, *J* = 8.8 Hz, 1H), 7.41–7.25 (m, 6H, aromatic + NH), 5.03 (s, 2H), 4.52–4.42 (m, 1H), 4.36 (dd, *J* = 8.99, 2.42 Hz, 1H), 4.18–4.11 (m, 1H), 3.93 (t, *J* = 8.51 Hz, 1H), 3.62 (s, 3H), 2.35–2.15 (m, 2H), 1.99–1.80 (m, 1H), 1.79–1.62 (m, 2H), 1.49–1.31 (m, 9H), 1.14–1.02 (m, 14H, CH₃ + Ile CH₂), 0.93–0.73 (m, 6H); HRMS (ESI) calcd for [C₃₂H₅₁N₃O₉ + Na]⁺, 644.3525, found: 644.3485 (M + 23).

Proteasome inhibitors

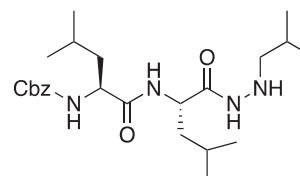


Benzyl ((S)-1-(((S)-1-hydrazineyl-4-methyl-1-oxopentan-2-yl)amino)-4-methyl-1-oxopentan-2-yl)carbamate (Cbz-Leu-Leu-NHNH₂). Cbz-Leu-Leu-OMe (7.0 g, 17.8 mmol) was dissolved in MeOH

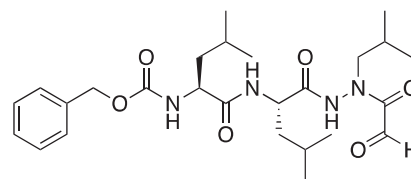
(150 ml) and hydrazine was added dropwise (5.59 ml, 178 mmol). The solution was allowed to stir for 18 h at RT. The solvent was removed *in vacuo* to afford Cbz-Leu-Leu-NHNH₂ as white solid (7.0 g, 99% yield). ¹H NMR (DMSO-d₆, 400 MHz): 9.18 (s, 1H), 7.86 (d, *J* = 9.01 Hz, 1H), 7.44 (d, *J* = 7.71 Hz, 1H), 7.44–7.27 (m, 5H), 5.03 (s, 2H), 4.32–4.23 (m, 1H), 4.10–4.00 (m, 1H), 1.68–1.51 (m, 2H), 1.50–1.28 (m, 4H), 0.82–0.88 (m, 12H).



Benzyl ((S)-1-(((S)-1-(2-(*E*)-2-methylpropylidene)hydrazineyl)-1-oxopentan-2-yl)amino)-1-oxopentan-2-yl)carbamate (Cbz-Leu-Leu-NHN = CHCH(CH₃)₂). Cbz-Leu-Leu-NHNH₂ (7.0 g, 17.8 mmol) was dissolved in dry THF (200 ml) followed by the addition of isobutyraldehyde (1.79 ml, 19.6 mmol) and catalytic acetic acid (1 drop). The solution was allowed to stir for 18 h at RT. The reaction was quenched with saturated NaHCO₃, extracted with DCM. The organic layer was dried over Na₂SO₄ and removed *in vacuo* to afford Cbz-Leu-Leu-NHN = CHCH(CH₃)₂ as a white solid (8 g, 99% yield). ¹H NMR (DMSO-d₆, 400 MHz): 10.81, 11.01 (s, 1H), 7.93, 7.77 (d, *J* = 8.3 Hz, 1H), 7.74 (d, 1H), 7.41 (d, 1H), 7.40–7.24 (m, 5H), 5.02 (s, 2H), 4.12–4.00 (m, 2H), 1.48–1.31 (m, 2H), 1.08–0.99 (m, 1H), 0.93–0.75 (m, 18H).

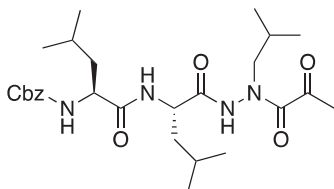


Benzyl ((S)-1-(((S)-1-(2-isobutylhydrazineyl)-4-methyl-1-oxopentan-2-yl)amino)-4-methyl-1-oxopentan-2-yl)carbamate (Cbz-Leu-Leu-NHNHCHCH(CH₃)₂). A solution of benzyl ((S)-1-(((S)-1-(2-(*E*)-2-methylpropylidene)hydrazineyl)-1-oxopentan-2-yl)amino)-1-oxopentan-2-yl)carbamate (1 g, 2.24 mmol) in MeOH (25 ml) was treated with acetic acid (0.2 ml) followed by sodium cyanoborohydride (170 mg, 2.69 mmol). The reaction was stirred at RT for 16 h, then the pH was adjusted to 10 by addition of 1 M NaOH. The solvent was removed *in vacuo*, and the residue was dissolved in DCM. The organic layer was washed with water, saturated brine, dried over Na₂SO₄ and concentrated *in vacuo* to afford the product as a white solid (874 mg, 1.95 mmol, 87% yield). ¹H NMR (DMSO-d₆, 400 MHz) δ: 9.25 (d, *J* = 4.2 Hz, 1H), 7.87 (d, *J* = 6.73 Hz, 1H), 7.30 (d, *J* = 7.32 Hz, 1H), 7.28–7.39 (m, 5H), 6.47 (d, 1H), 5.10 (s, 2H), 4.33–4.42 (m, 1H), 4.10–4.19 (m, 1H), 2.60 (m, 1H), 1.42–1.82 (m, 9H), 0.8–1.05 (m, 18H). HRMS (ESI) calcd for [C₂₄H₄₀NO₄ + Na]⁺ 471.2927, Found: 471.2950 (M + 23).

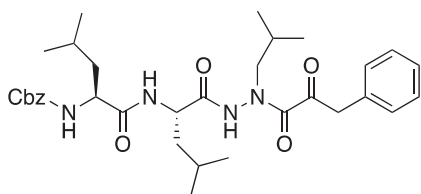


Compound 3: Benzyl ((S)-1-(((S)-1-(2-isobutyl-2-(2-oxoacetyl)hydrazineyl)-4-methyl-1-oxopentan-2-yl)amino)-4-methyl-1-oxopentan-2-yl)carbamate. (Cbz-Leu-Leu-ALeu-CHO). A 0 °C solution of benzyl

(*S*)-1-(((*S*)-1-(2-isobutylhydrazinyl)-4-methyl-1-oxopentan-2-yl)amino)-4-methyl-1-oxopentan-2-yl)carbamate (50 mg, 0.11 mmol) in dry DCM (2 ml) was treated with a solution of 2-oxoacetyl chloride (13 mg, 0.14 mmol) in DCM (0.5 ml) followed by DIPEA (0.02 ml, 0.14 mmol). The reaction was warmed to RT and stirred for 2 h. The reaction was quenched with H₂O and extracted with DCM. The organic layer was washed with saturated NaHCO₃, dried over Na₂SO₄ and concentrated *in vacuo*. The crude product was purified by silica gel chromatography (2% MeOH/DCM) to afford the product as a white solid (18 mg, 32% yield). ¹H NMR (DMSO-*d*₆, 400 MHz) δ 9.08 (s, 1H), 7.96 (s, 1H), 7.49–7.24 (m, 5H), 5.01 (s, 2H), 4.37–4.20 (m, 1H), 4.14–4.01 (m, 1H), 3.78–3.66 (m, 1H), 1.77–1.32 (m, 7H), 0.94–0.71 (m, 18H); ¹³C NMR (213 MHz, DMSO-*d*₆) δ (ppm) = 189.9, 173.9, 173.0, 157.6, 138.8, 130.2, 129.4, 129.3, 67.0, 54.6, 54.3, 42.5, 42.1, 25.3, 24.2, 23.2, 22.0; HRMS (ESI) calcd for [C₂₇H₄₄N₄O₇+Na]⁺ 559.3108, found 559.3098 (MeOH hemiacetal)



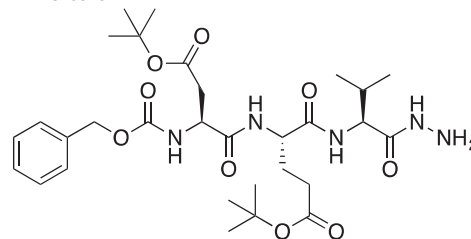
Compound 4: Benzyl ((*S*)-1-(((*S*)-1-(2-isobutyl-2-(2-oxopropionyl)hydrazinyl)-4-methyl-1-oxopentan-2-yl)amino)-4-methyl-1-oxopentan-2-yl)carbamate (Cbz-Leu-Leu-ALeu-COMe). A 0 °C solution of pyruvic acid (0.17 ml, 0.69 mmol) in DCM (10 ml) was treated with oxalyl chloride (0.06 ml, 0.72 mmol) followed by DMF (1 drop). The reaction mixture was warmed to RT and stirred 2 h. The solvent was removed *in vacuo*, and residue was dissolved in fresh DCM (5 ml) and chilled to 0 °C. A solution of benzyl ((*S*)-1-(((*S*)-1-(2-isobutylhydrazinyl)-4-methyl-1-oxopentan-2-yl)amino)-4-methyl-1-oxopentan-2-yl)carbamate (200 mg, 0.45 mmol) was added, followed by the addition of DIPEA (0.15 ml, 0.9 mmol). The reaction was stirred 1 h at 0 °C, then warmed to RT and stirred for an additional 16 h. The reaction mixture was diluted with H₂O and extracted with EtOAc. Organic extracts were dried over Na₂SO₄ and concentrated *in vacuo*. The crude product was purified by silica gel chromatography (20–40% EtOAc/Hexanes) to afford the product as a white solid (27 mg, 7.5% yield). ¹H NMR (DMSO-*d*₆, 400 MHz) δ 9.12 (s, 1H), 7.28–7.47 (m, 5H), 6.38 (d, *J* = 7.74 Hz, 1H), 5.24 (br s, 1H), 5.13 (d, *J* = 3.64 Hz, 2H), 4.45 (br s, 1H), 4.05–4.22 (m, 1H), 3.21–3.56 (m, 2H), 2.44 (s, 1H), 1.87–1.98 (m, 1H), 1.40–1.75 (m, 6H), 0.86–0.98 (m, 18H). ¹³C NMR (213 MHz, DMSO-*d*₆) δ (ppm) = 200.3, 174.1, 157.6, 138.8, 130.0, 129.5, 129.3, 67.0, 55.1, 54.5, 51.1, 42.3, 41.7, 28.9, 25.8, 24.7, 24.3, 23.2, 21.5; HRMS (ESI) calcd for [C₂₇H₄₂N₄O₆+Na]⁺ 541.2997, found: 541.2981.



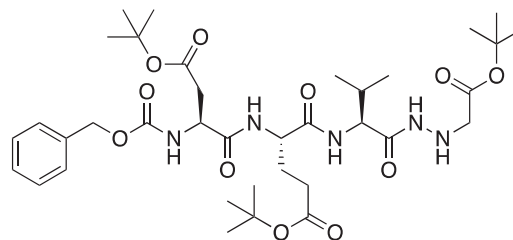
Compound 5: Benzyl ((*S*)-1-(((*S*)-1-(2-isobutyl-2-(2-oxo-3-phenylpropanoyl)hydrazinyl)-4-methyl-1-oxopentan-2-yl)amino)-4-methyl-1-oxopentan-2-yl)carbamate (Cbz-Leu-Leu-ALeu-COBn). To a solution of phenylpyruvic acid (73 mg, 0.44 mmol) in DCM (2 ml) oxalyl chloride (0.04 ml, 0.44 mmol) was added, followed by DMF (1 drop). The reaction mixture was stirred at RT for 2 h, then concentrated *in vacuo*. The resulting residue was dissolved in fresh

DCM (3 ml) and chilled to 0 °C. To this chilled solution was added a solution of benzyl ((*S*)-1-(((*S*)-1-(2-isobutylhydrazinyl)-4-methyl-1-oxopentan-2-yl)amino)-4-methyl-1-oxopentan-2-yl)carbamate (168 mg, 0.37 mmol) in DCM (1 ml) followed by DIPEA (0.13 ml, 0.74 mmol). The reaction was warmed to RT and stirred 16 h. The reaction mixture was diluted with H₂O and extracted with DCM. The organic layer was dried over Na₂SO₄ and concentrated *in vacuo*. The crude product was purified by silica gel chromatography (5% MeOH/DCM) and recrystallised from EtOAc/Et₂O to afford the pure product as a white solid (38 mg, 17% yield). ¹H NMR (CDCl₃, 400 MHz) δ: 8.92 (s, 1H), 7.27–7.41 (m, 10H), 7.15–7.20 (d, *J* = 7.07 Hz, 1H), 6.06 (d, *J* = 9.07 Hz, 1H), 5.04–5.14 (m, 2H), 4.31–4.92 (m, 1H), 3.92–4.20 (m, 3H, CH and Bn), 3.40–3.65 (s, 1H), 3.20–3.37 (m, 1H), 1.84–1.99 (m, 1H), 1.49–1.71 (m, 6H), 1.22–1.35 (m, 2H), 0.81–0.95 (m, 18H). ¹³C NMR (213 MHz, DMSO-*d*₆): δ (ppm) = 198.4, 173.9, 156.3, 137.6, 130.4, 130.1, 129.0, 128.9, 128.8, 128.7, 128.2, 128.1, 65.8, 53.9, 53.3, 42.2, 41.1, 24.6, 23.5, 23.3, 22.0, 21.9, 21.1, 20.3; HRMS (ESI) calcd for [C₃₃H₄₆N₄O₆+Na]⁺ 617.3316, found: 617.3308.

Caspase-3 inhibitors

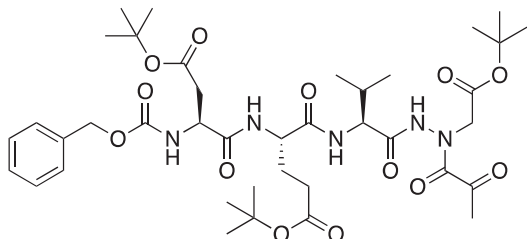


tert-Butyl (*S*)-4-((*S*)-2-(((benzyloxy)carbonyl)amino)-4-(*tert*-butoxy)-4-oxobutanamido)-5-(((*S*)-1-hydrazinyl-3-methyl-1-oxobutan-2-yl)amino)-5-oxopentanoate (Cbz-Asp(O*t*Bu)-Glu(O*t*Bu)-Val-NHNH₂). A solution of methyl (5*S*,8*S*,11*S*)-5-(2-(*tert*-butoxy)-2-oxoethyl)-8-(3-(*tert*-butoxy)-3-oxopropyl)-11-isopropyl-3,6,9-trioxo-1-phenyl-2-oxa-4,7,10-triazadodecan-12-oate (7.9 g, 12.7 mmol) in MeOH (80 ml) was treated with hydrazine (2.67 ml, 80 mmol). The reaction was stirred at RT for 18 h. The solvent and excess hydrazine were removed *in vacuo* to afford the product as a white solid. This was used for further transformations without additional purification (7.9 g, quantitative). ¹H NMR (DMSO-*d*₆, 400 MHz) δ: 9.16 (s, 1H), 7.98 (d, *J* = 8.1 Hz, 1H), 7.80 (d, *J* = 8.8 Hz, 1H), 7.64 (d, *J* = 8.3 Hz, 1H), 7.44–7.26 (m, 5H), 5.13–4.95 (m, 2H), 4.46–4.11 (m, 4H), 4.04 (t, *J* = 6.83 Hz, 1H), 2.69–2.36 (m, 2H), 2.30–2.14 (m, 2H), 1.96–1.81 (m, 2H), 1.52–1.30 (m, 18H), 0.89–0.76 (m, 6H); HRMS (ESI) calcd for [C₃₀H₄₈N₅O₉]⁺ 622.3447, found: 622.3415.

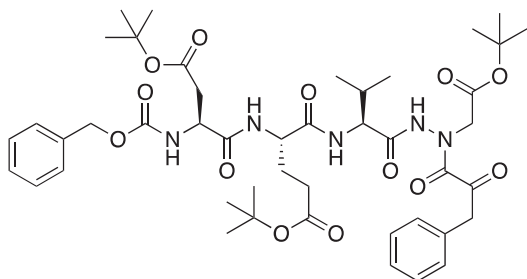


tert-Butyl (5*S*,8*S*,11*S*)-5-(2-(*tert*-butoxy)-2-oxoethyl)-8-(3-(*tert*-butoxy)-3-oxopropyl)-11-isopropyl-3,6,9,12-tetraoxo-1-phenyl-2-oxa-4,7,10,13,14-pentaazahexadecan-16-oate (Cbz-Asp(O*t*Bu)-Glu(O*t*Bu)-Val-NHNHCH₂CO₂*t*Bu). A –15 °C solution of *tert*-butyl (*S*)-4-((*S*)-2-(((benzyloxy)carbonyl)amino)-4-(*tert*-butoxy)-4-oxobutanamido)-5-(((*S*)-1-hydrazinyl-3-methyl-1-oxobutan-2-yl)amino)-5-oxopentanoate (1 g, 1.6 mmol) in DMF (6 ml) was treated with the

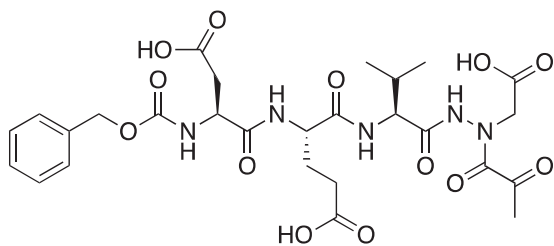
dropwise addition of *t*-butyl bromoacetate (0.26 ml, 1.76 mmol). The reaction was stirred for 30 min, then warmed to RT and stirred for 16 h. The solvent was removed *in vacuo*, and the residue was purified by silica gel chromatography (4% MeOH/DCM) to afford the title product as a white solid (115 mg, 10% yield); ^1H NMR (DMSO- d_6 , 400 MHz) δ : 9.48 (d, $J = 6.16$ Hz, 1H), 7.95 (d, $J = 7.44$ Hz, 1H), 7.85 (d, $J = 8.76$ Hz, 1H), 7.62 (d, $J = 8.76$ Hz, 1H), 7.47–7.22 (m, 5H), 5.18–5.11 (m, 1H), 5.10–4.98 (m, 2H), 4.51–4.19 (m, 2H), 4.11–3.99 (m, 1H), 3.41–3.38 (m, 2H), 2.27–2.16 (m, 2H), 1.96–1.69 (m, 5H), 1.46–1.34 (m, 27H), 0.86–0.77 (m, 6H).



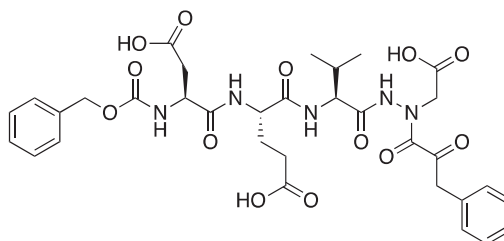
tert-Butyl (5*S*,8*S*,11*S*)-5-(2-(*tert*-butoxy)-2-oxoethyl)-8-(3-(*tert*-butoxy)-3-oxopropyl)-11-isopropyl-3,6,9,12-tetraoxo-14-(2-oxopropanoyl)-1-phenyl-2-oxa-4,7,10,13,14-pentaazahexadecan-16-oate (Cbz-Asp(O*t*Bu)-Glu(O*t*Bu)-Val-AAsp(O*t*Bu)-COMe). Prepared following the general procedure for coupling of aza-peptide to pyruvic acid as previously described; (36 mg, 29% yield); ^1H NMR (CDCl₃, 400 MHz) δ : 9.02 (s, 1H), 7.90 (d, $J = 4.99$ Hz, 1H), 7.46–7.33 (m, 5H), 6.11–5.99 (m, 1H), 5.22–5.10 (m, 2H), 4.55–4.45 (m, 1H), 4.37–4.25 (m, 2H), 4.24–4.16 (m, 1H), 3.01–2.74 (m, 2H), 2.57–2.39 (m, 2H), 2.37 (s, 3H), 2.33–2.24 (m, 1H), 2.19–1.99 (m, 2H), 1.49–1.44 (m, 27H), 0.97–0.92 (m, 6H); HRMS (ESI) calcd for [C₃₉H₅₉N₅O₁₃+Na]: 828.4002, found: 828.3984.



tert-Butyl (5*S*,8*S*,11*S*)-5-(2-(*tert*-butoxy)-2-oxoethyl)-8-(3-(*tert*-butoxy)-3-oxopropyl)-11-isopropyl-3,6,9,12-tetraoxo-14-(2-oxo-3-phenylpropanoyl)-1-phenyl-2-oxa-4,7,10,13,14-pentaazahexadecan-16-oate (Cbz-Asp(O*t*Bu)-Glu(O*t*Bu)-Val-AAsp(O*t*Bu)-COBn). This product was prepared following the general procedure for coupling of an aza-peptide to phenylpyruvic acid as previously described; (19 mg, 18% yield); ^1H NMR (DMSO- d_6 , 400 MHz) δ : 11.07 (s, 1H), 8.00 (d, $J = 8.3$ Hz, 1H), 7.93 (d, $J = 7.7$ Hz, 1H), 7.60 (d, $J = 8.3$ Hz, 1H), 7.40–7.15 (m, 11H), 5.12–4.96 (m, 2H), 4.41–4.28 (m, 2H), 4.21–4.12 (m, 1H), 4.10–3.96 (m, 2H), 2.70–2.57 (m, 1H), 2.47–2.39 (m, 1H), 2.26–2.14 (m, 2H), 1.94–1.80 (m, 2H), 1.77–1.65 (m, 2H), 1.44 (s, 9H), 1.37–1.32 (m, 18H), 0.81–0.75 (m, 6H); HRMS (ESI) calcd for [C₄₅H₆₃N₅O₁₃+Na]: 904.4315, found: 904.4282.

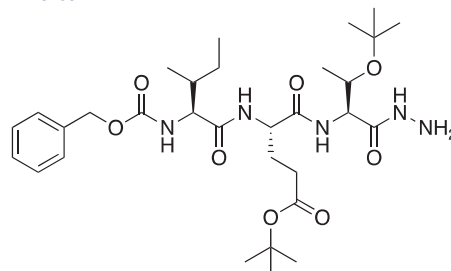


Compound 6: (5*S*,8*S*,11*S*)-8-(2-Carboxyethyl)-5-(carboxymethyl)-11-isopropyl-3,6,9,12-tetraoxo-14-(2-oxopropanoyl)-1-phenyl-2-oxa-4,7,10,13,14-pentaazahexadecan-16-oic acid (Cbz-Asp-Glu-Val-AAsp-COME). A solution of *tert*-butyl (5*S*,8*S*,11*S*)-5-(2-(*tert*-butoxy)-2-oxoethyl)-8-(3-(*tert*-butoxy)-3-oxopropyl)-11-isopropyl-3,6,9,12-tetraoxo-14-(2-oxopropanoyl)-1-phenyl-2-oxa-4,7,10,13,14-pentaazahexadecan-16-oate (36 mg, 0.045 mmol) in DCM (0.5 ml) was treated with trifluoroacetic acid (0.5 ml). The reaction was stirred 2 h, then concentrated to dryness *in vacuo* to afford the product as a white solid (27 mg, 95% yield). ^1H NMR (DMSO- d_6 , 400 MHz) δ : 11.02 (br s, 1H), 8.17–7.78 (m, 2H), 7.73–7.53 (d, $J = 8.0$ Hz, 1H), 7.42–7.29 (m, 5H), 5.04 (s, 2H), 4.42–4.29 (m, 2H), 4.13 (t, $J = 6.8$ Hz, 1H), 2.70–2.57 (m, 2H), 2.48–2.43 (m, 1H), 2.29–2.18 (m, 5H), 1.96–1.82 (m, 2H), 0.82 (d, $J = 6.4$ Hz, 6H). ^{13}C NMR (213 MHz, DMSO- d_6): δ (ppm) = 199.7, 175.7, 173.4, 173.2, 172.9, 172.8, 172.5, 170.4, 170.0, 157.5, 138.6, 130.1, 129.5, 129.4, 67.2, 57.8, 53.3, 53.0, 50.3, 37.9, 31.7, 31.6, 29.1, 20.5, 19.6; HRMS (ESI) calcd for [C₂₇H₃₅N₅O₁₃+Na]⁺ 660.2124, found 660.2116 (M + 23).



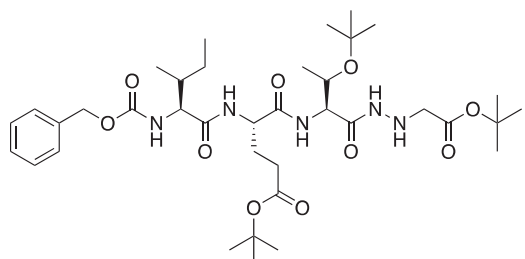
Compound 7: (5*S*,8*S*,11*S*)-8-(2-Carboxyethyl)-5-(carboxymethyl)-11-isopropyl-3,6,9,12-tetraoxo-14-(2-oxo-3-phenylpropanoyl)-1-phenyl-2-oxa-4,7,10,13,14-pentaazahexadecan-16-oic acid (Cbz-Asp-Glu-Val-AAsp-COBn). *tert*-Butyl (5*S*,8*S*,11*S*)-5-(2-(*tert*-butoxy)-2-oxoethyl)-8-(3-(*tert*-butoxy)-3-oxopropyl)-11-isopropyl-3,6,9,12-tetraoxo-14-(2-oxo-3-phenylpropanoyl)-1-phenyl-2-oxa-4,7,10,13,14-pentaazahexadecan-16-oate (18 mg, 0.02 mmol) was dissolved in a 1:1 DCM/trifluoroacetic acid mixture (1.5 ml). The mixture was stirred for 2.5 h, then solvent was removed, and product was dried *in vacuo* to give the title compound as a white solid (13.6 g, 95%). ^1H NMR (DMSO- d_6 , 400 MHz) δ : 11.06 (s, 1H), 8.02–7.91 (m, 2H), 7.61 (d, $J = 8.0$ Hz, 1H), 7.42–7.15 (m, 10H), 5.03 (s, 2H), 4.44–4.27 (m, 3H), 4.21–4.12 (m, 2H), 4.06–3.94 (m, 3H), 2.70–2.60 (m, 1H), 2.80–2.18 (m, 2H), 1.95–1.84 (m, 2H), 1.80–1.70 (m, 1H), 0.84–0.70 (m, 6H); ^{13}C NMR (213 MHz, DMSO- d_6): δ (ppm) = 199.3, 173.4, 173.3, 173.0, 172.5, 170.4, 157.5, 138.6, 131.2, 131.7, 131.6, 130.0, 129.9, 129.5, 129.4, 128.6, 67.2, 57.8, 53.4, 53.0, 50.3, 46.8, 37.9, 31.7, 26.4, 20.7, 19.5; HRMS (ESI) calcd for [C₃₃H₃₉N₅O₁₃+Na]⁺ 736.2437, found: 736.2415 (M + 23).

Caspase-6 inhibitor

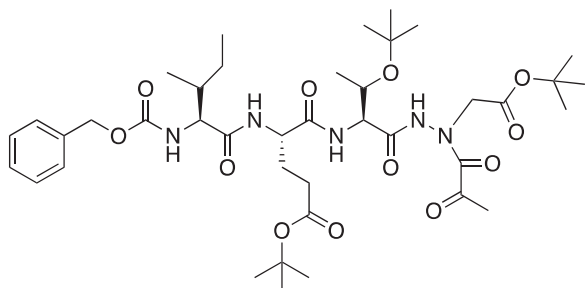


tert-Butyl (S)-4-((2*S*,3*R*)-2-(((benzyloxy)carbonyl)amino)-3-methylpentanamido)-5-(((2*S*,3*S*)-3-(*tert*-butoxy)-1-hydrazinyl)-1-oxobutan-2-yl)amino)-5-oxopentanoate (Cbz-Ile-Glu(O*t*Bu)-Thr(O*t*Bu)-NHNH₂).

A solution of methyl (5S,8S,11S)-8-(3-(*tert*-butoxy)-3-oxopropyl)-11-((*S*)-1-(*tert*-butoxy)ethyl)-5-((*R*)-*s*-butyl)-3,6,9-trioxo-1-phenyl-2-oxa-4,7,10-triazadodecan-12-oate (2.08 g, 3.35 mmol) in MeOH (10 ml) was treated with hydrazine (5.3 ml, 169.8 mmol). The reaction mixture was stirred at RT for 16 h. Excess hydrazine and MeOH were removed *in vacuo* to afford the product as a white solid (9.80 g, 98% yield). ¹H NMR (DMSO-*d*₆, 400 MHz) δ : 8.88 (s, 1H), 8.12 (d, 1H), 7.46 (d, 1H), 7.46–7.35 (m, 6H), 5.02 (s, 2H), 4.38 (m, 1H), 4.25 (s, 2H) 4.15 (m, 1H), 3.40 (m, 2H), 2.30–2.12 (m, 2H), 1.93–1.79 (m, 1H), 1.76–1.63 (m, 2H), 1.13–1.06 (s, 9H), 1.10 (s, 11H), 0.99–0.93 (m, 3H), 0.77–0.82 (m, 6H); HRMS (ESI) calcd for [C₃₁H₅₁N₅O₈+Na]⁺, 644.3638, found: 644.3624 (M + 23).

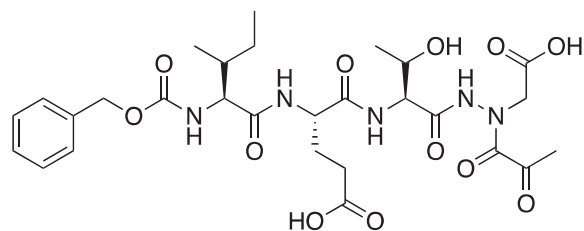


tert-Butyl (5S,8S,11S)-8-(3-(*tert*-butoxy)-3-oxopropyl)-11-((*S*)-1-(*tert*-butoxy)ethyl)-5-((*R*)-*s*-butyl)-3,6,9,12-tetraoxo-1-phenyl-2-oxa-4,7,10,13,14-pentaazahexadecan-16-oate (Cbz-Ile-Glu(OtBu)-Thr(OtBu)-NHNHCH₂CO₂tBu). A -15 °C solution of *tert*-butyl (S)-4-((2S,3R)-2-(((benzyloxy)carbonyl)amino)-3-methylpentanamido)-5-(((2S,3S)-3-(*tert*-butoxy)-1-hydrazinyl-1-oxobutan-2-yl)amino)-5-oxopentanoate (1.174 g, 1.89 mmol) in dry DMF (100 ml) was treated with NMM (0.26 ml, 1.89 mmol) and left to stir 15 min. The solution was then treated with *t*-butyl bromoacetate (0.42 ml, 2.835 mmol) and allowed to stir for 30 min at -15 °C. Following, the solution was allowed to stir while gradually warming to RT for 16 h. The reaction mixture was concentrated *in vacuo* and the crude product was purified by silica gel chromatography (10% MeOH/DCM) to afford the product as a white solid (0.4641 g, 0.6306 mmol, 33% yield). ¹H NMR (DMSO-*d*₆, 400 MHz) δ : 9.14 (d, *J* = 5.8 Hz, 1H), 8.11 (d, *J* = 8.0 Hz, 1H), 7.55 (d, *J* = 8.5 Hz, 1H), 7.36 (m, 6H, aromatic CH + NH), 5.12 (q, *J* = 5.1 Hz, 1H), 5.02 (s, 2H), 4.42–4.31 (m, 1H), 4.18 (dd, *J* = 8.6, 3.7 Hz, 1H), 3.92–3.88 (m, 2H, α CH + CH Thr), 3.38 (s, 2H), 2.36–2.09 (m, 2H), 1.96–1.79 (m, 1H), 1.77–1.58 (m, 2H), 1.47–1.34 (m, 20H, Ile CH₂ + CH₃), 1.10 (s, 9H), 1.00–0.93 (m, 3H), 0.90–0.74 (m, 6H); HRMS (ESI) calcd for [C₃₇H₆₁N₅O₁₀ + Na]⁺ 758.4318, found 758.4301 (M + 23).



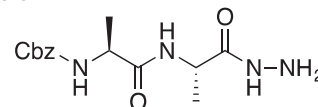
tert-Butyl (5S,8S,11S)-8-(3-(*tert*-butoxy)-3-oxopropyl)-11-((*S*)-1-(*tert*-butoxy)ethyl)-5-((*R*)-*s*-butyl)-3,6,9,12-tetraoxo-14-(2-oxopropanoyl)-1-phenyl-2-oxa-4,7,10,13,14-pentaazahexadecan-16-oate (Cbz-Ile-Glu(OtBu)-Thr(OtBu)-AAsp(OtBu)-COMe). A solution of pyruvic acid (0.02 ml, 0.20 mmol) in dry DCM (50 ml) was treated with oxalyl chloride (0.02 ml, 0.217 mmol) followed by 1 drop of DMF (cat). The reaction was stirred at RT for 3 h, then concentrated *in vacuo*. The resulting residue was dissolved in dry DCM (50 ml), chilled to 0 °C and treated dropwise with a solution of *tert*-butyl (5S,8S,11S)-

8-(3-(*tert*-butoxy)-3-oxopropyl)-11-((*S*)-1-(*tert*-butoxy)ethyl)-5-((*R*)-*s*-butyl)-3,6,9,12-tetraoxo-1-phenyl-2-oxa-4,7,10,13,14-pentaazahexadecan-16-oate (100 mg, 0.136 mmol) in dry DCM (20 ml) and DIPEA (0.05 ml, 0.272 mmol). The reaction was stirred for 16 h at RT. The reaction was quenched with H₂O, and washed with saturated brine. The organic layer was dried over Na₂SO₄ and concentrated *in vacuo*. The crude product was purified by silica gel chromatography (10% MeOH/DCM) to afford product as a white solid (22.8 mg, 21% yield). ¹H NMR (DMSO-*d*₆, 400 MHz) δ : 10.77 (s, 1H), 8.05 (d, *J* = 7.9 Hz, 1H), 7.75 (d, *J* = 7.8 Hz, 1H), 7.42–7.24 (m, 6H, aromatic CH + NH), 5.02 (s, 2H), 4.54–4.44 (m, 1H), 4.27 (dd, *J* = 8.0, 4.5 Hz, 1H), 3.92 (t, *J* = 8.1 Hz, 1H), 3.95–3.89 (m, 1H), 2.23 (s, 5H), 1.85 (m, 1H), 1.70 (m, 2H), 1.88–1.39 (m, 18H), 1.11 (s, 11H), 0.95 (m, 3H), 0.86–0.74 (m, 6H); HRMS (ESI) calcd for [C₄₀H₆₃N₅O₁₂+Na]⁺ 828.4373, found 828.4360 (M + 23).

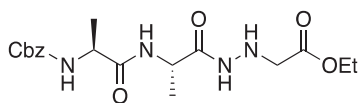


Compound **8**: (5S,8S,11S)-5-((*R*)-*s*-butyl)-8-(2-carboxyethyl)-11-((*S*)-1-hydroxyethyl)-3,6,9,12-tetraoxo-14-(2-oxopropanoyl)-1-phenyl-2-oxa-4,7,10,13,14-pentaazahexadecan-16-oic acid (Cbz-Ile-Glu-Thr-AAAsp-COMe). *tert*-butyl (5S,8S,11S)-8-(3-(*tert*-butoxy)-3-oxopropyl)-11-((*S*)-1-(*tert*-butoxy)ethyl)-5-((*R*)-*s*-butyl)-3,6,9,12-tetraoxo-14-(2-oxopropanoyl)-1-phenyl-2-oxa-4,7,10,13,14-pentaazahexadecan-16-oate (22.8 mg, 0.028 mmol) was dissolved in 1:1 DCM/TFA (20 ml) at 0 °C and allowed to stir 30 min then warmed to RT and stirred an additional 1 h. The solution was concentrated *in vacuo* to afford the product as a white solid (15.8 mg, 85% yield). ¹H NMR (DMSO-*d*₆, 400 MHz) δ : 10.82 (s, 1H), 8.00 (d, *J* = 7.99 Hz, 1H), 7.80 (d, *J* = 7.96 Hz, 1H), 7.35 (m, 6H), 5.02 (s, 2H), 4.89 (m, 1H), 4.39 (m, 1H), 4.17 (m, 1H), 3.92 (m, 2H), 2.24 (s, 3H), 1.90 (m, 1H), 1.70 (m, 2H), 1.39 (m, 2H), 1.22 (s, 2H), 0.99 (m, 3H), 0.80 (m, 6H); ¹³C NMR (175 MHz, DMSO-*d*₆) δ (ppm) = 201.4, 178.6, 176.2, 172.2, 170.1, 167, 163, 149.1, 145.3, 135.9, 130.0, 129.9, 129.4, 67.1, 65.3, 62.3, 60.8, 57.4, 36.6, 31.6, 25.9, 21.2, 18.2, 12.7, 11.8. HRMS (ESI) calcd for [C₂₈H₃₉N₅O₁₂+Na]⁺ 660.2487, found 660.2485 (M + 23).

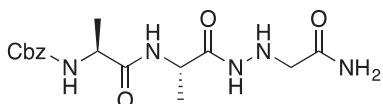
Legumain inhibitors



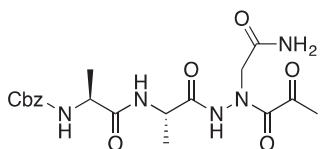
Benzyl ((*S*)-1-(((*S*)-1-hydrazinyl-1-oxopropan-2-yl)amino)-1-oxopropan-2-yl)carbamate (Cbz-Ala-Ala-NHNH₂). To a solution of methyl ((benzyloxy)carbonyl)-*L*-alanine (*L*-Ala-OMe) (2.0 g, 6.4 mmol) in MeOH (50 ml), hydrazine (2.12 ml, 64 mmol) was added dropwise. The reaction was allowed to stir at RT for 18 h. MeOH and excess hydrazine were removed *in vacuo* and the resulting white solid was washed with EtOAc to afford a white solid (1.68 g, 5.4 mmol, 85% yield). ¹H NMR (DMSO-*d*₆, 400 MHz) δ : 9.05 (s, 1H), 7.90 (d, *J* = 7.7 Hz, 1H), 7.42 (d, *J* = 7.6 Hz, 1H), 7.41–7.26 (m, 5H), 4.97–5.07 (m, 2H), 4.20–4.26 (m, 2H), 4.04–4.11 (m, 2H), 1.19 (s, 3H), 1.18 (s, 3H).



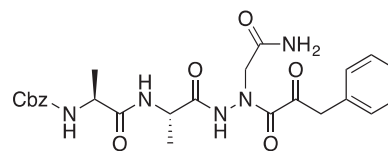
Ethyl ((S)-2-(((S)-2-((benzyloxy)carbonyl)amino)propanamido)propanamido)glycinate (Cbz-Ala-Ala-NHNHCH₂CO₂Et). To solution of benzyl ((S)-1-(((S)-1-hydrazinyl-1-oxopropan-2-yl)amino)-1-oxopropan-2-yl)carbamate (1.68 g, 5.4 mmol) and NMM (0.65 ml, 5.9 mmol) in DMF (8 ml) at -10°C ethyl bromoacetate (0.65 ml, 5.9 mmol) was added dropwise. The reaction was stirred at -10°C for 30 min, then warmed to RT and stirred for an additional 16 h. The reaction was then concentrated *in vacuo*, and the resulting residue was purified by silica gel chromatography (1:9 MeOH/DCM) to afford a white solid (375 mg, 20% yield). ¹H NMR: (DMSO-d₆, 400 MHz) δ 9.34 (d, J = 5.8 Hz, 1H), 7.92 (d, J = 7.58 Hz, 1H), 7.41–7.47 (d, J = 7.7 Hz, 1H), 7.28–7.41 (m, 5H), 5.18 (q, J = 4.94 Hz, 1H), 5.02 (s, 2H), 4.18–4.26 (m, 1H), 4.01–4.14 (m, 2H), 3.48 (d, J = 5.24 Hz, 2H), 1.35–1.44 (m, 3H), 1.15–1.22 (m, 6H).



Benzyl ((S)-1-(((S)-1-(2-(2-amino-2-oxoethyl)hydrazinyl)-1-oxopropan-2-yl)amino)-1-oxopropan-2-yl)carbamate (Cbz-Ala-Ala-NHNHCH₂CONH₂). A 7 M solution of ammonia in MeOH (13.5 ml, 94.5 mmol) was added to a 0°C solution of ethyl ((S)-2-(((S)-2-((benzyloxy)carbonyl)amino)propanamido)propanamido)glycinate (375 mg, 0.95 mmol) in DMF (0.4 ml). NaCN (5 mg, 0.095 mmol) was added, and the reaction vessel was sealed. The mixture was stirred at 0°C for 2 h, then warmed to RT and stirred for 48 h. The reaction was concentrated *in vacuo* and the product was precipitated with 9:1 DCM/MeOH to afford a white solid (343 mg, 98% yield). ¹H NMR (DMSO-d₆, 400 MHz) δ 9.33 (s, 1H), 7.98 (d, J = 7.0 Hz, 1H), 7.30–7.47 (m, 5H), 7.12 (s, 1H), 5.22 (t, J = 4.13 Hz, 1H), 4.97–5.08 (m, 2H), 4.15–4.24 (m, 1H), 4.01–4.11 (m, 1H), 3.20 (d, J = 5.23 Hz, 2H), 1.20 (s, 3H), 1.18 (s, 3H).



Compound **10**: Benzyl ((S)-1-(((S)-1-(2-(2-amino-2-oxoethyl)-2-(2-oxopropanoyl)hydrazinyl)-1-oxopropan-2-yl)amino)-1-oxopropan-2-yl)carbamate (Cbz-Ala-Ala-AAsn-COMe). A 0°C solution of pyruvic acid (0.15 ml, 0.62 mmol) in DCM (10 ml) was treated with oxalyl chloride (0.06 ml, 0.66 mmol), followed by one drop of DMF (cat). The reaction was stirred at 0°C for 30 min, then warmed to RT and stirred an additional 1.5 h. To this mixture was added DIPEA (0.14 ml, 0.82 mmol) followed by a solution of benzyl ((S)-1-(((S)-1-(2-(2-amino-2-oxoethyl)hydrazinyl)-1-oxopropan-2-yl)amino)-1-oxopropan-2-yl)carbamate (150 mg, 0.41 mmol) in 1:2 DCM/DMF (1 ml). The reaction was stirred for 16 h, then concentrated *in vacuo* and purified by silica chromatography (1:9 MeOH/DCM) to afford a white solid (24 mg, 13% yield). ¹H NMR (DMSO-d₆, 400 MHz) δ : 10.41 (s, 1H), 9.05 (s, 1H), 8.11–8.00 (m, 1H), 7.55–7.26 (m, 7H), 5.03 (s, 2H), 4.13–4.05 (m, 2H), 3.18 (d, J = 5.24 Hz, 2H), 2.03–1.98 (m, 3H), 1.55–1.42 (m, 6H); HRMS (ESI) calcd for [C₁₉H₂₅N₅O₇+Na]⁺ 458.1652, Found: 458.1634 (M + 23).



Compound **11**: Benzyl ((S)-1-(((S)-1-(2-(2-amino-2-oxoethyl)-2-(2-oxo-3-phenylpropanoyl)hydrazinyl)-1-oxopropan-2-yl)amino)-1-oxopropan-2-yl)carbamate (Cbz-Ala-Ala-AAsn-COBn). A solution of phenylpyruvic acid (172 mg, 1.05 mmol) in DCM (3 ml) was treated with oxalyl chloride (0.09 ml, 1.05 mmol), followed by DMF (1 drop), and the reaction was stirred for 1.5 h at RT, then concentrated *in vacuo*. The resulting residue was taken up in fresh DCM (5 ml). To this solution was added a solution of benzyl ((S)-1-(((S)-1-(2-(2-amino-2-oxoethyl)hydrazinyl)-1-oxopropan-2-yl)amino)-1-oxopropan-2-yl)carbamate (80 mg, 0.21 mmol) in DCM (1.5 ml), followed by DIPEA (0.07 ml, 0.21 mmol). The reaction was stirred at RT for 16 h, then concentrated *in vacuo* and purified by silica gel chromatography (2–10% MeOH/DCM) then recrystallised from EtOAc/Et₂O to afford the product as a white solid (19 mg, 0.037 mmol, 18% yield). ¹H NMR (DMSO-d₆, 400 MHz) δ : 8.13 (d, J = 7.89 Hz, 1H), 7.17–7.40 (m, 12H, ArH and NH₂), 4.94–5.08 (m, 2H), 4.17–4.31 (m, 1H), 4.05–4.13 (m, 1H), 4.00 (s, 2H), 1.05–1.30 (m, 6H); ¹³C NMR (175 MHz, DMSO-d₆) δ (ppm) = 197.0, 168.4, 161.8, 157.4, 130.1, 130.0, 129.97, 129.94, 129.9, 129.5, 129.4, 67.0, 60.0, 59.5, 51.5, 45.9, 45.5, 19.8; HRMS (ESI) calcd for [C₂₅H₂₉N₅O₇+Na]⁺ 534.1965, Found: 534.1975 (M + 23).

Proteasome kinetic assay

Human 20S proteasome, 700 kDa, was purchased from Boston Biochem (50 μg , 2 μM (1.4 mg/mL) in 50 mM HEPES buffer (pH 7.6, 100 mM NaCl, 1 mM DTT). Assay buffer was prepared as follows: 20 mM HEPES buffer pH 7.8, 0.5 mM EDTA, 0.037% SDS. Proteasome specific substrate Suc-LLVY-AMC was purchased from Boston Biochem and used as a fluorogenic substrate; λ_{ex} = 380 nm, λ_{em} = 442 nm. 18 μL of 2 μM proteasome solution was diluted with 425 μL H₂O to make a 0.06 μM stock enzyme solution for kinetic assays. In a 96-well plate suitable for fluorometric assays was added 86 μL assay buffer, 2 μL inhibitor, 2 μL enzyme substrate, and 10 μL enzyme stock solution (0.06 nM enzyme concentration in well). Fluorescence at 442 nm was monitored for 10 min. The enzyme activity was measured in triplicate at varying concentrations of inhibitor (0, 25, 50, 100 μM in DMSO) and substrate (10, 20, 50, 100 μM in DMSO for K_i measurements, and 100 μM for IC₅₀ measurements) by converting the slope of the plot of fluorescence intensity at 442 nm vs time for time points between 4 and 8 min using Beer-Lambert's law. IC₅₀ values were obtained from non-linear fitting of the data to a competitive inhibition model using GraphPad Prism 7.0 software. The proteasome $\beta 5$ chymotrypsin-like active site activity assay was performed as previously described⁴¹.

Caspase kinetic assay

Caspase-3 and caspase-6 were generous gifts from Prof. Guy Salvesen's laboratory and then used at Ohio State University. Caspase activities were measured in 100 mM HEPES, 10% sucrose, 0.1% CHAPS, 10 mM DTT, pH 7.5 at 37 $^{\circ}\text{C}$. To 5,000 μL of this buffer, 100 μL of freshly prepared 1 M DTT and 4,900 μL DI H₂O were added resulting in the caspase assay buffer. Studies were performed at 37 $^{\circ}\text{C}$.

Caspase-3

Caspase-3 specific substrate Ac-DEVD-AMC was purchased from Cayman Chemical Company and used as fluorogenic substrate; $\lambda_{\text{ex}} = 353 \text{ nm}$, $\lambda_{\text{em}} = 442 \text{ nm}$. 2 μL of 33 μM caspase-3 solution was diluted with 4998 μL caspase assay buffer to make a 13.2 nM enzyme stock solution. In a 96-well plate suitable for fluorometric assays, 80 μL assay buffer, 5 μL inhibitor, 5 μL enzyme substrate (0.1 mM), and 10 μL enzyme stock solution were added. Fluorescence at 442 nm was monitored for 10 min. The enzyme activity was measured in triplicate at varying concentrations of inhibitor (0, 25, 50, 100 μM in DMSO) and substrate (0.1 mM in DMSO) by converting the slope of the plot of fluorescence intensity at 442 nm vs time for the time points between 4 and 8 min using Beer-Lambert's law. IC_{50} values were obtained from non-linear fitting of the data to a competitive inhibition model using GraphPad Prism 7.0 software.

Caspase-6

Caspase-6 specific substrate Ac-VEID-AFC was purchased from ChemCruz and used as a fluorogenic substrate; $\lambda_{\text{ex}} = 400 \text{ nm}$, $\lambda_{\text{em}} = 505 \text{ nm}$. To 45 μL of assay buffer, 5 μL of the 19.7 μM enzyme was added. This resulting enzyme solution was further diluted 1:5 with assay buffer resulting in a 0.32 μM solution. In a 96-well plate suitable for fluorometric assays was added 80 μL assay buffer, 5 μL inhibitor, 5 μL enzyme substrate (0.1 mM), and 10 μL enzyme stock solution (32 nM enzyme concentration in well). The enzyme activity was measured in triplicate at varying concentrations of inhibitor (0, 25, 50, 100 μM in DMSO) and substrate (0.1 mM in DMSO) by converting the slope of the plot of fluorescence intensity at 442 nm vs time for the time points between 4 and 8 min using Lambert-Beer's law. IC_{50} values were obtained from non-linear fitting of the data to a competitive inhibition model using GraphPad Prism 7.0 software.

Legumain kinetic assay

Schistosoma mansoni and *Ixodes ricinus* legumain zymogens were expressed in the yeast, *Pichia pastoris*, as described^{36,42}. Legumain kinetic assay details: zymogens were activated for 3 h (*Ir*) or overnight (*Sm*) at room temperature in 0.1 M Na-Ac pH 4.0; 5 mM DTT. Activities were measured in 0.1 M Na-Ac pH 5.5; 2.5 mM DTT, 0.1% PEG 6000 buffer. The substrate used was Cbz-AAN-AMC with 50 μM final concentration in the assay. Inhibitors were prepared in DMSO (1% DMSO in activity assay). Measurements were taken with an incubation period of 10 min at room temperature, and the enzyme activity was measured in triplicate. Asparaginyl Endopeptidase (AE) activity assay was performed as previously described⁷.

Cathepsin B kinetic assay

Human Liver Cathepsin B (purified) was purchased from Enzo Life Sciences (in 50 mM sodium acetate, pH 5.0 containing 1 mM EDTA). The Cathepsin B activity assay is performed in 0.1 M phosphate, 1.25 mM EDTA, 0.01% Brij, pH 6.0 buffer at 37 °C. Cathepsin B specific substrate Cbz-Arg-Arg-AMC was purchased from Sigma Aldrich and used as fluorogenic substrate; $\lambda_{\text{ex}} = 380 \text{ nm}$, $\lambda_{\text{em}} = 442 \text{ nm}$. The assay buffer was prepared as follows 0.1 M K_3PO_4 , 1.25 mM EDTA, 0.01% Brij 35 with a pH of 6 was made with 1 mM DTT added immediately prior to assay. To 100 μL of assay buffer, 5 μL of the received 0.427 mg/mL Cathepsin B solution was added. The resulting solution was further diluted 1:6 of Cathepsin B to assay buffer for a final concentration of 2.9 $\mu\text{g}/\text{mL}$. In a 96-well

plate suitable for fluorometric assays was added 85 μL assay buffer, 5 μL inhibitor, 5 μL enzyme substrate, and 5 μL enzyme stock solution (0.145 $\mu\text{g}/\text{mL}$ enzyme concentration in well). The enzyme activity was measured in triplicate at varying concentrations of inhibitor (0, 62.5, 125 μM in DMSO) and substrate (0.1 mM in DMSO) by converting the slope of the plot of fluorescence intensity at 442 nm vs time for the time points between 4 and 8 min using Lambert-Beer's law. IC_{50} values were obtained from non-linear fitting of the data to a competitive inhibition model using GraphPad Prism 7.0 software.

α -Chymotrypsin kinetic assay

α -Chymotrypsin from bovine pancreas, type II lyophilised powder, >40 units/mg protein activity was purchased from Sigma Aldrich and was tested in 50 mM sodium phosphate, pH 7.5 buffer at 37 °C. To prepare the enzyme stock solution, 1.6 mg α -chymotrypsin was dissolved in 1,600 μL assay buffer. The resulting stock enzyme solution was further diluted 1:200 stock to assay buffer for a final stock concentration of 5 $\mu\text{g}/\text{mL}$. α -Chymotrypsin specific substrate Suc-LLVY-AMC was purchased from Boston Biochem and used as a fluorogenic substrate; $\lambda_{\text{ex}} = 353 \text{ nm}$, $\lambda_{\text{em}} = 442 \text{ nm}$. In a 96-well plate suitable for fluorometric assays was added 80 μL assay buffer, 5 μL inhibitor, 5 μL enzyme substrate, and 10 μL enzyme stock solution (0.5 $\mu\text{g}/\text{mL}$ enzyme concentration in well). The enzyme activity was measured in triplicate at varying concentrations of inhibitor (0, 50, 125 μM in DMSO) and substrate (0.1 mM in DMSO), by converting the slope of the plot of fluorescence intensity at 442 nm vs time for the time points between 4 and 8 min using Lambert-Beer's law. IC_{50} values were obtained from non-linear fitting of the data to a competitive inhibition model using GraphPad Prism 7.0 software.

Protein expression and purification

The expression and purification of caspase-3 was performed as previously described^{43,44} with several modifications. The cDNA encoding the caspase-3 sequence with the addition of an N-terminal 6xHis-tag followed by a TEV protease recognition sequence was codon optimised for expression in *E. coli* (GenScript) and placed in a pET15b vector (Invitrogen). The protein was expressed in *E. coli* at 30 °C for 24 h after 200 mM IPTG induction. Cells were pelleted by centrifugation and lysed by sonication. The lysate was cleared by centrifugation and purified by Ni-NTA (GE Healthcare) and Q-Sepharose (GE Healthcare) chromatography. TEV protease (1.25 mg) was added to the purified protein during overnight dialysis at 4 °C and the TEV protease and free His-tag were removed by reverse Ni-NTA purification. Any remaining impurities were removed and the buffer was exchanged by size-exclusion chromatography on a Superdex 200 Increase column equilibrated with 20 mM Tris, 20 mM NaCl, 10 mM DTT, pH = 7.5 yielding protein with purity >95% by SDS-PAGE. The protein was concentrated to 5 mg/mL by ultrafiltration (10 kDa MWCO, EMD Millipore), flash frozen, and stored at -80 °C until ready to use.

Crystallisation and structure determination

The protein was inhibited by adding 20 mM Cbz-DEVD-COME inhibitor in DMSO to a final concentration of 2.1 mM giving a final concentration of 4 mg/ml caspase-3/inhibitor complex. Protein crystallisation was performed by hanging-drop vapour diffusion at 298 K with 1:1 ratio of mother liquor (50 mM sodium citrate, 15.33% PEG 6000, 7.5% glycerol, 10 mM DTT, pH = 6.2) to the

protein/inhibitor complex. Crystals were observed within one day and reached their maximum dimensions within 7 days. Crystals were cryoprotected in a 1:4 solution of glycerol:mother liquor and frozen on the instrument in the cryo-stream at 100 K. X-ray diffraction data were collected in-house on a Compact HomeLab X-ray diffractometer (Rigaku) with MicroMax 003i generator, AFC-11 4-axis goniometer, and Pilatus 200 K detector.

Diffraction images were indexed, integrated, and scaled with HKL3000 (HKL Research, Inc.) in the P2₁2₁ space group with a maximum resolution of 2.73 Å. Phases were determined by molecular replacement with 2H5I⁴³ as a model using Phaser-MR in the Phenix software package⁴⁵. Coordinates and restraints for the sulphur-bound ligand were created using eLBOW⁴⁶ and PRODRG (GlycoBioChem Ltd.) and modified with REEL⁴⁷. Refinement was performed using phenix.refine⁴⁸ in the Phenix software package and all coordinates and electron density maps were visualised using winCOOT⁴⁹. Statistical information for the solved structure can be viewed in [Supplemental information](#).

Results and discussion

Chemical synthesis

The general preparation of aza-peptide aldehydes and ketones involves the synthesis of the substituted hydrazide precursor⁵ and its coupling to oxoacetyl chloride (prepared *in situ* with thionyl chloride) for aldehydes and to methyl or benzyl pyruvic acid chlorides for ketones, respectively.

The tripeptidyl inhibitor synthesis begins with an isobutyl chloroformate mediated coupling between the methyl ester of the P₂ amino acid and the carboxybenzyl protected P₃ amino acid ([Figure 2](#)).

From the P₃-P₂ dipeptide, the P₁ aza-amino acid is added by, first, the addition of excess hydrazine to the methyl ester to furnish the corresponding hydrazide **1** in quantitative yield ([Figure 3](#)), followed by reductive amination with an appropriate aldehyde to install the P₁ side chain. The aza-leucine derivative was synthesised by a two-step reductive amination, first reacting the hydrazide Cbz-Leu-Leu-NHNH₂ and isobutyraldehyde to afford a hydrazide intermediate, which was subsequently reduced with sodium cyanoborohydride to effectively install the isobutyl side chain on the hydrazide to form the aza-leucine intermediate **2** in good yield ([Figure 3](#)).

With the synthesis of the inhibitor backbones complete, the final step was the coupling of the aza-peptide intermediate to the

electrophilic carbonyl warheads ([Figure 4](#)). The aza-peptide aldehyde inhibitor was prepared by conversion of glyoxylic acid to the corresponding acid chloride by refluxing in thionyl chloride, and then coupling this intermediate to the aza-peptide hydrazides in a manner analogous to the synthesis of the ketone inhibitors ([Figure 4\(A\)](#)).

Initially, we proposed a methyl and a benzyl ketone to explore the tolerance of functional groups in the S₁' pocket where the ketone R' group was anticipated to reside. We have chosen the methyl and benzyl groups for two reasons. (a) The methyl group is the smallest group possible for our proposed aza-peptide ketone design, and (b) the phenyl group, if tolerated, can be derivatised further to make more specific interactions at the prime site. Coupling of the warheads was performed by conversion of readily available pyruvic acid or phenylpyruvic acid to the corresponding acid chloride intermediates via reaction with oxalyl chloride, and then acyl substitution of the acid chloride with the aza-peptide hydrazide intermediates, thereby yielding the final aza-peptide ketones ([Figure 4\(B\)](#)). These two described methods were used for the synthesis of the aza-peptide aldehyde **3** as well as ketones **4** and **5**, as shown in [Figure 4\(C\)](#).

A series of caspase-3 aza-peptide ketone inhibitors as well as one caspase-6 aza-peptide ketone bearing a P₁ aza-aspartate residue were synthesised and evaluated ([Figure 5](#)).

The tri-peptide hydrazides Z-Asp(O^tBu)-Glu(O^tBu)-Val-NHNH₂ and Z-Ile-Glu(O^tBu)-Thr(O^tBu)-NHNH₂ were synthesised using the general peptide coupling and hydrazide formation conditions described for the proteasome inhibitors above. The aza-aspartate residue was synthesised according to [Figure 6](#). Nucleophilic substitution of the hydrazide with *tert*-butyl bromoacetate gave the *tert*-butyl aspartate protected intermediates of the general structure **9**. Analogous warhead coupling methods to those described in [Figure 4](#) were then used, followed by a trifluoroacetic acid deprotection of the *tert*-butyl groups, affording the final inhibitors **6**, **7**, and **8**.

Inhibitors were also designed and synthesised to target the legumain protease. The clan CD cysteine protease, legumain, has a preference to cleave substrates after an asparagine amino acid residue and has the optimal substrate sequence Cbz-Ala-Ala-Asn⁵⁰. The aza-peptide ketone inhibitors **10** and **11** depicted in [Figure 7](#), targeting inhibition of legumain, were synthesised.

The synthesis of legumain inhibitors **10** and **11** was performed by adaptation of the previous syntheses. The alanine-alanine dipeptide hydrazide **12** intermediate ([Figure 8](#)) was synthesised using an isobutyl chloroformate peptide coupling method,

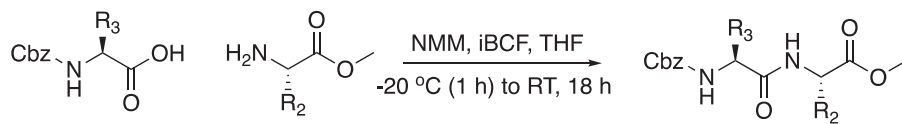


Figure 2. General peptide coupling approach.

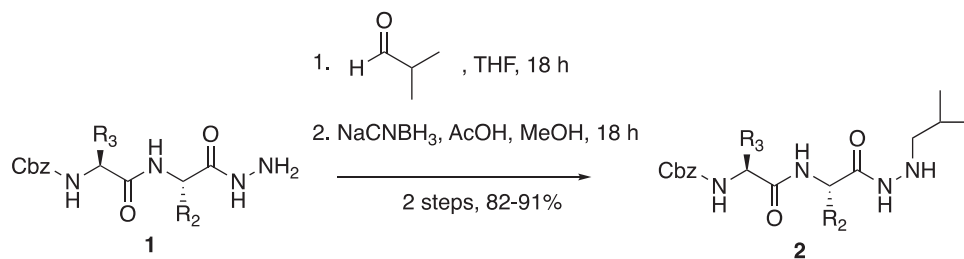


Figure 3. Substituted hydrazide precursor synthesis.

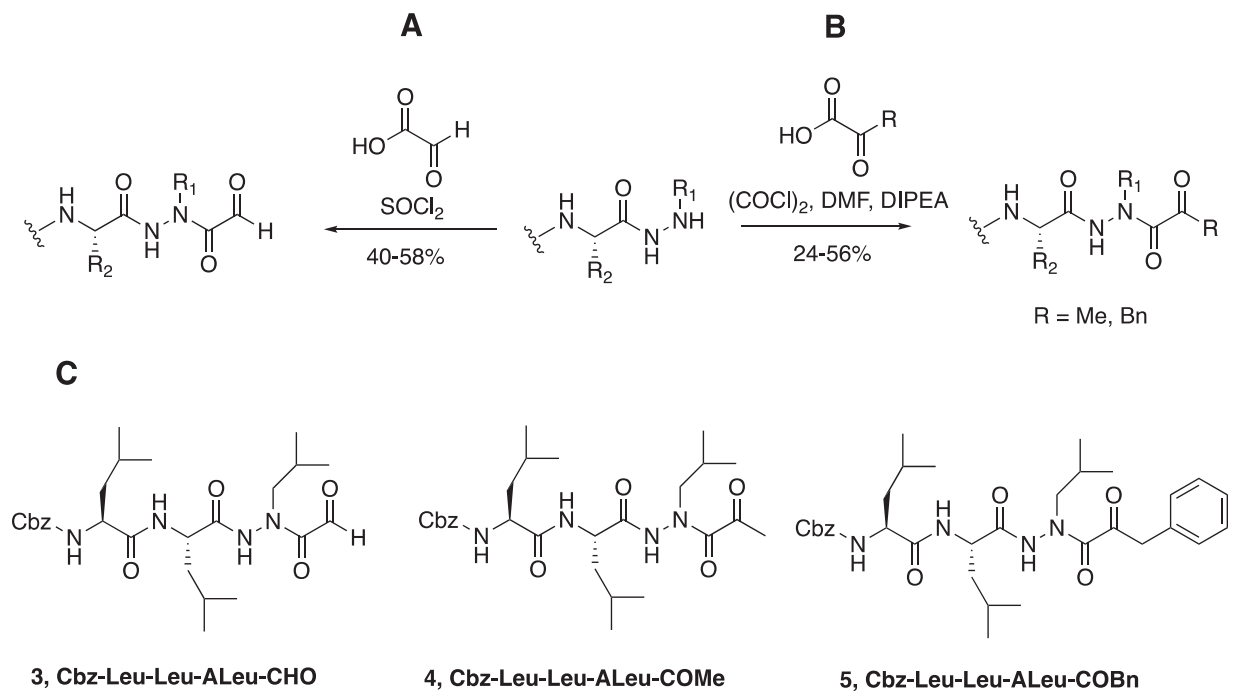


Figure 4. (A) Coupling procedure for aza-peptide aldehyde warhead. (B) Coupling procedure for aza-peptide ketone warhead. (C) Library of synthesised aza-peptide aldehyde and ketone inhibitors for the proteasome.

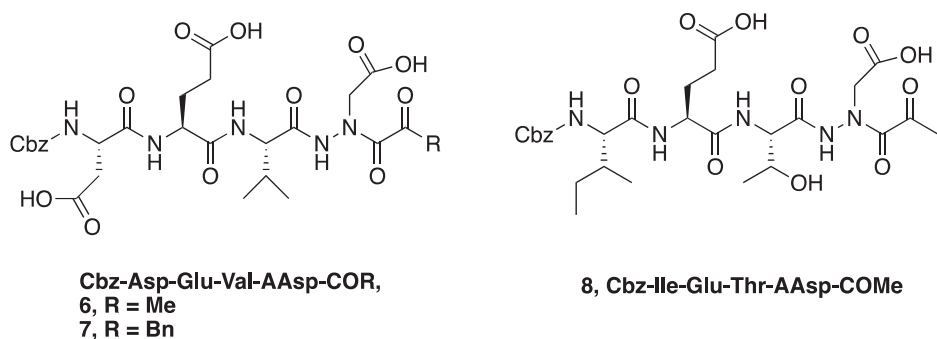


Figure 5. Aza-peptide ketone inhibitors designed for caspase-3 and -6.

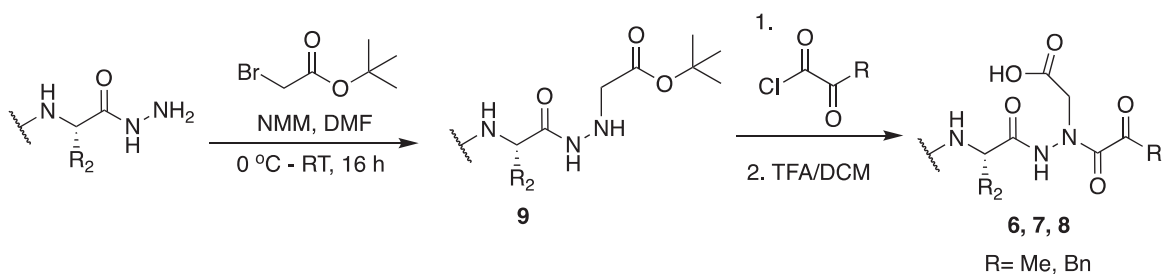


Figure 6. Synthesis of the aza-aspartate caspase inhibitors.

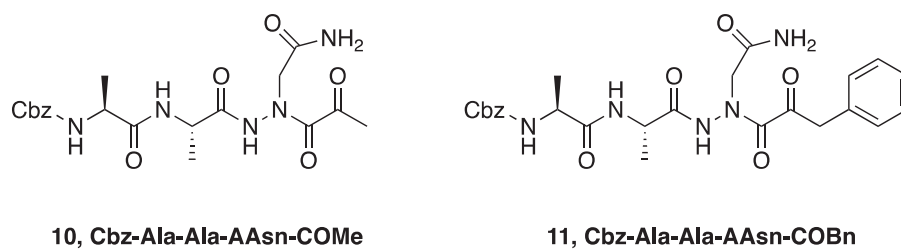


Figure 7. Aza-peptide ketone inhibitors designed for the clan CD legumain protease.

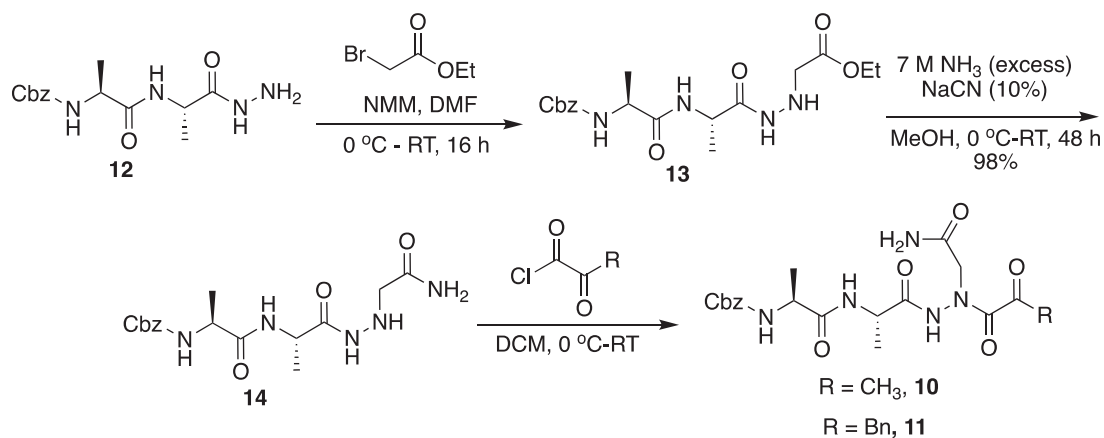


Figure 8. Synthesis of aza-asparagine legumain inhibitors.

followed by the reaction of the resulting methyl ester with hydrazine. The intermediate **12** was subjected to reaction with ethyl bromoacetate to afford the alkylated hydrazide **13**. Amidation of the ethyl ester was carried out with ammonia in a sealed pressure tube to afford **14**, as previously reported⁵. These precursors were subsequently coupled with the methyl or benzyl keto-warhead to give the final inhibitors **10** and **11**.

In vitro inhibition

We synthesised a total of eight final compounds. Each compound was characterised by ¹H and ¹³C nuclear magnetic resonance spectra and electrospray ionisation mass spectra (see the Materials and Methods section). The results of the inhibition of the various aza-peptide aldehydes and ketones are summarised in Tables 1–3.

Compounds **3**, **4** and **5** are designed to target the β_5 , chymotrypsin-like (CT-L) active site of the human 20S proteasome, and thus are based on the ideal tripeptidyl sequence Leu-Leu-Leu⁵¹. To our knowledge, this is the first study where a chemical electrophilic warhead bearing an aza-P1 residue was designed and tested with the proteasome. Compounds **3**, **4** and **5** showed inhibition in the mid- μ M range, suggesting that the proteasome active site can actually tolerate the aza-modification at the P₁ position (Table 1). Inhibition rates by the aldehyde **3** and ketones **4** and **5** seemed fairly close with the aldehyde **3** being slightly more potent with an IC₅₀ value of 9.02 μ M. The benzyl group of the ketone inhibitor **5** was well accommodated at the prime site for this warhead motif with an IC₅₀ value of 10.11 μ M, allowing further derivatisation on the aromatic ring for more potency and specificity. The overall performance of our compounds, particularly compound **3**, can be directly compared to the commercially available aldehyde inhibitor MG132 (Cbz-Leu-Leu-Leu-CHO). MG132 is a very potent, but non-selective, proteasome inhibitor. In our assay, we have determined the K_i value of MG132 of the β_5 , chymotrypsin-like (CT-L) active site of the 20S proteasome as 14.28 \pm 3.06 nM. This value compares well with the previously reported K_i values of MG132 as 2–4 nM⁵², “few nanomolar”⁵³, and of the close analog MG115 (Cbz-Leu-Leu-Nle-CHO) as 21 nM⁵⁴ using the same substrate Suc-LLVY-AMC as in our assay.

Compounds **6** and **7** were designed as tetrapeptides to target human caspase-3 with the ideal sequence Asp-Glu-Val-Asp and compound **8** targets human caspase-6 with its optimal sequence Ile-Glu-Thr-Asp as caspases require a minimum of four amino acids in their recognition sequence²⁶. Compounds **6**, **7**, and **8** show low-to-mid μ M range inhibition with their target enzyme, where the best inhibitor is ketone **6** with an IC₅₀ value of 7.74 μ M against

Table 1. Inhibition of β_5 active site of the human 20S proteasome by aza-peptide aldehydes and ketones

Compound	Structure	IC ₅₀ (μ M)
3	Cbz-Leu-Leu-AlLeu-CHO	9.02 \pm 1.82
4	Cbz-Leu-Leu-AlLeu-COMe	14.56 \pm 2.39
5	Cbz-Leu-Leu-AlLeu-COBn	10.11 \pm 4.49
MG132	Cbz-Leu-Leu-Leu-CHO	0.0142 \pm 0.003 ^a

^aThis is a K_i value.

Table 2. Inhibition of human caspase-3 and caspase-6 by aza-peptide ketones

Compound	Structure	IC ₅₀ (μ M)	
		Caspase-3	Caspase-6
6	Cbz-Asp-Glu-Val-AAsp-COMe	7.74 \pm 1.88	51.93 \pm 10.64
7	Cbz-Asp-Glu-Val-AAsp-COBn	13.36 \pm 4.61	64.23 \pm 45.40
8	Cbz-Ile-Glu-Thr-AAsp-COMe	122 \pm 83.31	9.08 \pm 3.02

Table 3. Inhibition of *S. mansoni* and *I. ricinus* legumains by aza-peptide ketones

Compound	Structure	IC ₅₀ (μ M)	
		<i>S. mansoni</i>	<i>I. ricinus</i>
10	Cbz-Ala-Ala-AAsn-COMe	>100	>100
11	Cbz-Ala-Ala-AAsn-COBn	22.23 \pm 4.21	17.82 \pm 11.17

caspase-3 (Table 2). As expected, the caspase-3 specific compounds **6** and **7** show less activity against caspase-6; however, due to the strict P₁ Asp requirement for cleavage for all caspases, it is a challenge to obtain highly selective inhibition among different caspase family members. Likewise, compound **8** inhibits caspase-6 with an IC₅₀ value of 9.08 μ M, 13 times more effectively than it inhibits caspase-3, emphasising the importance of the preference in caspase-3 for the P₄ Asp residue. Within caspase-3 and -6, the benzyl compound **7** demonstrates the lowest inhibition for both enzymes, with IC₅₀ values of 13.36 and 64.23 μ M, respectively.

Compounds **10** and **11** were tested for their ability to inhibit the legumain proteases *S. mansoni* and *I. ricinus* and displayed IC₅₀ values in the mid- μ M range (Table 3). Compound **11** inhibited the *I. ricinus* and *S. mansoni* legumains with IC₅₀ values of 17.82 μ M and 22.23 μ M, respectively, suggesting a favourable aromatic interaction on the prime site for both enzymes. The aza-asparagine methyl ketone **10** inhibitor did not show inhibition

towards either of the legumains at the highest concentration tested (100 μM).

In addition to screening all of the compounds with their respective target enzymes, we also tested them for possible cross-reactivities with human liver cathepsin B and bovine pancreas

Table 4. Cross-reactivity of human cathepsin B and bovine pancreas α -chymotrypsin with aza-peptide aldehydes and ketones

Compound	Structure	Inhibition (μM)	
		Cathepsin B	α -Chymotrypsin
3	Cbz-Leu-Leu-ALeu-CHO	NI ^a	NI ^a
4	Cbz-Leu-Leu-ALeu-COMe	NI ^a	NI ^a
5	Cbz-Leu-Leu-ALeu-COBn	ND	ND
6	Cbz-Asp-Glu-Val-AAsp-COMe	NI ^b	NI ^b
7	Cbz-Asp-Glu-Val-AAsp-COBn	NI ^b	NI ^b
8	Cbz-Ile-Glu-Thr-AAsp-COMe	NI ^c	NI ^c
10	Cbz-Ala-Ala-AAsn-COMe	ND	NI ^b
11	Cbz-Ala-Ala-AAsn-COBn	ND	ND

NI: no inhibition; ND: not determined; NI up to ^a62.5 μM , ^b50 μM , ^c125 μM .

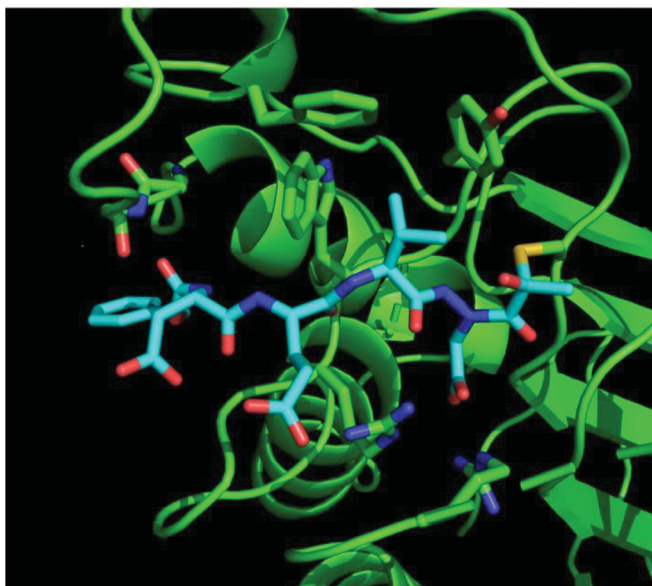


Figure 9. Caspase-3 in complex with Cbz-Asp-Glu-Val-AAsp-COMe (Compound 6). Compound 6 is observed residing in the active site of caspase-3 at a resolution of 2.73 \AA after thiohemiacetal covalent-bond formation to the methyl ketone warhead of 6.

α -chymotrypsin (Table 4). Cathepsin B was chosen to represent the clan CA type of cysteine proteases, and α -chymotrypsin representing the general chymotrypsin fold of serine proteases. The literature comparison compound, MG132 potently inhibits calpains and various lysosomal cathepsins with K_i values of 5–12 nM⁵⁴ in addition to the proteasome⁵². Our compounds, on the other hand, showed no inhibition of either cathepsin B or α -chymotrypsin at concentrations 50 μM and higher, suggesting no *in vitro* cross-reactivity and high selectivity among different families of proteases (see the Materials and Methods section for more details). While *in vitro* and *in vivo* selectivities do not always correlate, initial observation of *in vitro* selectivity is valuable information, and then, one can interpret subsequent *in vivo* behaviour in light of *in vitro* data more precisely. The initial *in vitro* selectivity is a desired and promising asset to these compounds, rendering their further development into potential drug candidates both compelling and exciting.

Binding mode and mechanism of inhibition

We determined the X-ray crystal structure of caspase-3 in complex with our aza-peptide methyl ketone inhibitor 6, Cbz-Asp-Glu-Val-AAsp-COMe (Figure 9).

We observed a similar binding mode at the active site in accordance with the previously determined X-ray structures of caspase-3 with inhibitors such as Ac-Asp-Glu-Val-Asp-H⁵⁵ and Ac-Asp-Val-Ala-Asp-FMK⁵⁶. In all of these structures, key hydrogen-bonding interactions between the P1 Asp side chain of the inhibitor with two Arg side chains (Arg64 and Arg207 in our structure) on the protein backbone is the determinant of the strict P1 Asp specificity. We also observed that the P3 Glu forms a hydrogen bond with Arg207 as well. In addition, the P2 Val side chain is well accommodated by the Phe256, Trp206 and Tyr204 aromatic rings. Most importantly, we observed the nucleophilic addition of the active site Cys163 of caspase-3 at the carbonyl carbon resulting in a tetrahedral thiohemiacetal adduct (Figure 10).

Based on our observations from the X-ray crystal structure of caspase-3 in complex with compound 6, we propose that the inhibition mechanism by the proteasome proceeds via a nucleophilic attack of the deprotonated Thr-O⁻ at the carbonyl carbon of our warhead, thereby forming a reversible tetrahedral hemiacetal adduct 15 as shown in Figure 11. Similarly, we propose that inhibition by the other clan CD cysteine proteases, such as the

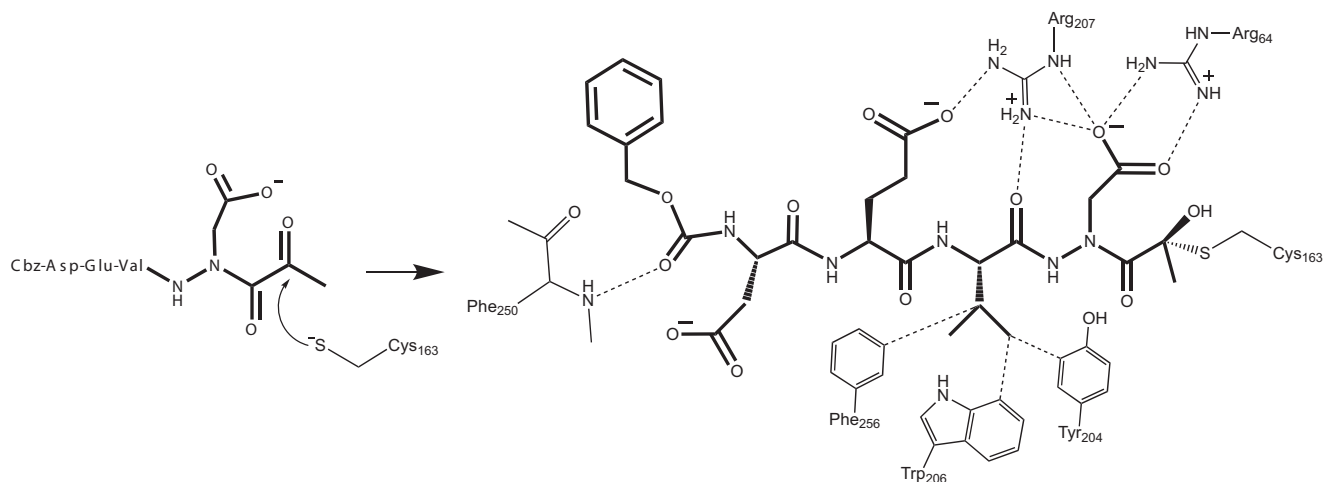


Figure 10. Mechanism of inhibition of caspase-3 by the aza-peptide methyl ketone inhibitor Cbz-Asp-Glu-Val-AAsp-COMe (Compound 6). The inhibitor ketone carbonyl carbon is the site of nucleophilic addition by the active-site Cys163 sulphur atom, resulting in covalent bond formation.

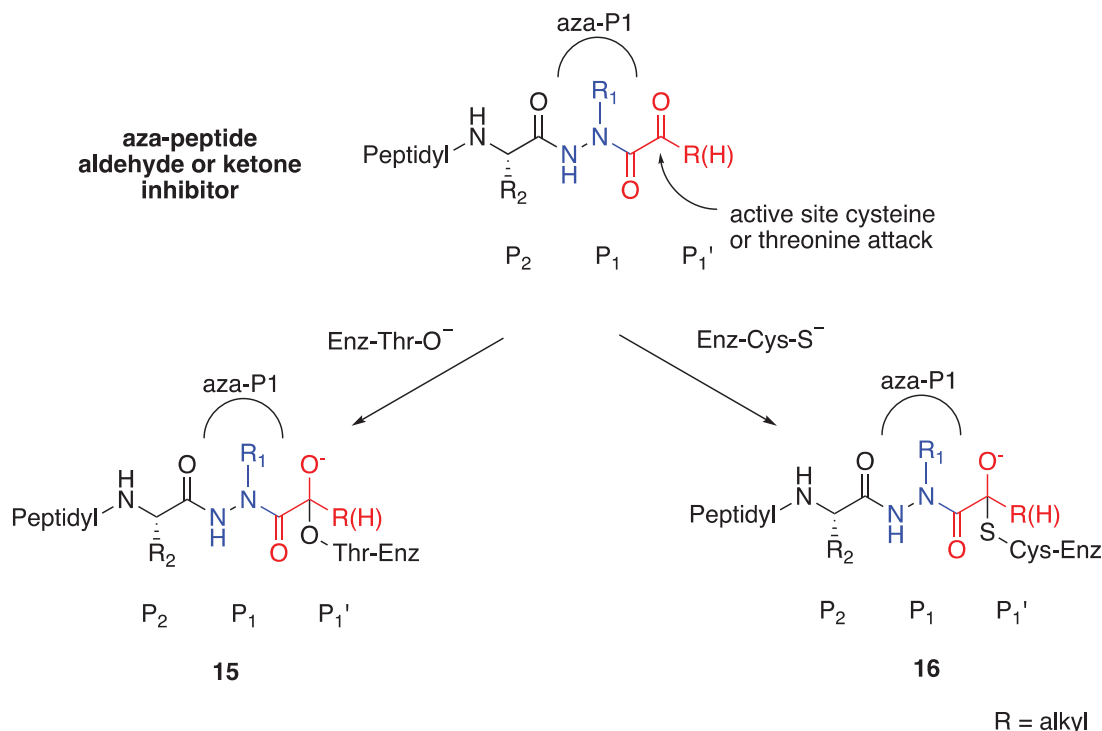


Figure 11. Proposed mechanism of inhibition by aza-peptide aldehydes and ketones reacting with (a) the proteasome and with (b) other clan CD cysteine proteases. The carbonyl carbon is expected to be the site of attack by nucleophilic residues: a Thr-O with the proteasome and a Cys-S with clan CD cysteine proteases.

legumains, occurs by nucleophilic addition of the deprotonated active site Cys-S⁻, similarly forming the reversible tetrahedral thiohemiacetal adduct **16**.

Conclusions

In summary, we have developed a new class of peptidyl protease inhibitors bearing an aza-P1 residue that are effective against the proteasome, caspases and legumains. The inhibitors were designed and synthesised based on their ideal substrate sequence. The tripeptide Leu-Leu-Aza-Leu sequence was chosen to target the $\beta 5$, chymotrypsin-like active site of the proteasome. Likewise, Asp-Glu-Val-Aza-Asp, Ile-Glu-Thr-Aza-Asp and Ala-Ala-Aza-Asn were chosen as preferred substrate sequences for the caspases-3, and -6 and legumains, respectively.

Eight novel compounds were synthesised and evaluated for their ability to inhibit their respective target proteases *in vitro*, and were shown to be low-to-mid- μ M range inhibitors. Each inhibitor was also tested for cross-reactivity with cathepsin B and α -chymotrypsin, and resulted in no inhibition ($>50 \mu$ M). X-ray crystallographic data with caspase-3 revealed a tetrahedral adduct with compound **6**, providing insight into the mechanism of inhibition. The micromolar range of inhibitory potency for these aza-peptide aldehydes and ketones could be attributed to the fact that the point of the nucleophilic attack is one chemical bond away towards the C-terminus from where the scissile bond normally would reside (Figure 1). However, it is also advantageous that the proteasome, caspases-3, and -6, and legumains still tolerate this aza-P1 design, whereas the classical cysteine protease cathepsin B and α -chymotrypsin do not. These differences provide an opportunity for tuneability as well as selectivity, and possibly less off-target reactivity as observed for bortezomib, carfilzomib and ixazomib.

We hypothesise that the potency of aza-peptide ketones can be improved by increasing the inductive effect on the prime site's

alkyl group which will render the ketone carbonyl to be more electrophilic. Our future, second generation compounds will be designed and synthesised accordingly. Overall, the *in vitro* selectivity and reversible nature of these inhibitors makes them more desirable drug candidates, as any possible cross reactivity would be reversible, arguably resulting in less severe side effects.

Acknowledgements

The authors acknowledge Dr. James H. McKerrow (UC-San Diego) in facilitating the logistics regarding the legumain assays to be performed.

Disclosure statement

The authors report no conflict of interest.

Funding

O.D.E. and C.M.H. acknowledge funding from The Ohio State University Technology Commercialisation Office Accelerator Award [GRT00051721]. G.S.S. acknowledges grant support from NIGMS [R01GM099040]. D.S. acknowledges funding from the Centre for Research of Pathogenicity and Virulence of Parasites [no. CZ.02.1.01/0.0/0.0/16_019/0000759], funded by the European Regional Development Fund (ERDF) and Ministry of Education, Youth, and Sport, Czech Republic (MEYS). Research at the CDIPD was funded in part by the NIH-NIAID award [R21AI126296] to C.R.C.

References

- Proulx C, Sabatino D, Hopewell R, et al. Azapeptides and their therapeutic potential. *Future Med Chem* 2011;3: 1139–64.
- Aubin S, Martin B, Delcros JG, et al. Retro hydrazino-azapeptides as peptidomimetics of proteasome inhibitors. *J Med Chem* 2005;48:330–4.
- Graybill TL, Ross MJ, Gauvin BR, et al. Synthesis and evaluation of azapeptide-derived inhibitors of serine and cysteine proteases. *Bioorg Med Chem Lett* 1992;2:1375–80.
- Ekici OD, Götz MG, James KE, et al. Aza-peptide michael acceptors: a new class of inhibitors specific for caspases and other clan cd cysteine proteases. *J Med Chem* 2004;47: 1889–92.
- Asgian JL, James KE, Li ZZ, et al. Aza-peptide epoxides: a new class of inhibitors selective for clan cd cysteine proteases. *J Med Chem* 2002;45:4958–60.
- James KE, Asgian JL, Li ZZ, et al. Design, synthesis, and evaluation of aza-peptide epoxides as selective and potent inhibitors of caspases-1, -3, -6, and -8. *J Med Chem* 2004;47: 1553–74.
- Götz MG, James KE, Hansell E, et al. Aza-peptidyl michael acceptors. A new class of potent and selective inhibitors of asparaginyl endopeptidases (legumains) from evolutionarily diverse pathogens. *J Med Chem* 2008;51:2816–32.
- Löser R, Frizler M, Schilling K, Gütschow M. Azadipeptide nitriles: highly potent and proteolytically stable inhibitors of papain-like cysteine proteases. *Angew Chem Int Ed Engl* 2008;47:4331–4.
- Schmitz J, Beckmann AM, Dudic A, et al. 3-Cyano-3-aza- β -amino acid derivatives as inhibitors of human cysteine cathepsins. *ACS Med Chem Lett* 2014;5:1076–81.
- Bochtler M, Ditzel L, Groll M, et al. The proteasome. *Annu Rev Biophys Biomol Struct* 1999; 28:295–317.
- Ciechanover A. The ubiquitin-proteasome proteolytic pathway. *Cell* 1994;79:13–21.
- Dahlmann B. Role of proteasomes in disease. *BMC Biochem* 2007;8(Suppl 1): S3.
- Delcros JG, Floc'h MB, Prigent C, Arlot-Bonnemains Y. Proteasome inhibitors as therapeutic agents: current and future strategies. *Curr Med Chem* 2003;10:479–503.
- Zhou HJ, Aujay MA, Bennett MK, et al. Design and synthesis of an orally bioavailable and selective peptide epoxyketone proteasome inhibitor (pr-047). *J Med Chem* 2009;52: 3028–38.
- Demo SD, Kirk CJ, Aujay MA, et al. Antitumor activity of pr-171, a novel irreversible inhibitor of the proteasome. *Cancer Res* 2007;67:6383–91.
- Adams J. The development of proteasome inhibitors as anti-cancer drugs. *Cancer Cell* 2004;5:417–21.
- Meregalli C. An overview of bortezomib-induced neurotoxicity. *Toxics* 2015;3:294–303.
- Manasanch EE, Orłowski RZ. Proteasome inhibitors in cancer therapy. *Nat Rev Clin Oncol* 2017;14:417–33.
- Park JE, Miller Z, Jun Y, et al. Next-generation proteasome inhibitors for cancer therapy. *Transl Res* 2018;198:1–16.
- Waxman AJ, Clasen S, Hwang WT, et al. Carfilzomib-associated cardiovascular adverse events a systematic review and meta-analysis. *JAMA Oncol* 2018;4:e174519.
- Kumar S, Moreau P, Hari P, et al. Management of adverse events associated with ixazomib plus lenalidomide/dexamethasone in relapsed/refractory multiple myeloma. *Br J Haematol* 2017;178:571–82.
- Salvesen GS. Caspases and apoptosis. *Essays Biochem* 2002; 38:9–19.
- Salvesen GS. Caspases: opening the boxes and interpreting the arrows. *Cell Death Differ* 2002;9:3–5.
- Schulz JB, Weller M, Moskowitz MA. Caspases as treatment targets in stroke and neurodegenerative diseases. *Ann Neurol* 1999;45:421–9.
- Thornberry NA, Peterson EP, Zhao JJ, et al. Inactivation of interleukin-1 beta converting enzyme by peptide (acyloxy)-methyl ketones. *Biochemistry* 1994;33:3934–40.
- Thornberry NA, Rano TA, Peterson EP, et al. A combinatorial approach defines specificities of members of the caspase family and granzyme b. Functional relationships established for key mediators of apoptosis. *J Biol Chem* 1997;272: 17907–11.
- Thornberry NA. The caspase family of cysteine proteases. *Br Med Bull* 1997;53:478–90.
- Thornberry NA. Caspases: key mediators of apoptosis. *Chem Biol* 1998;5:R97–103.
- Graham RK, Ehrnhoefer DE, Hayden MR. Caspase-6 and neurodegeneration. *Trends Neurosci* 2011;34:646–56.
- Ishii S. Legumain: asparaginyl endopeptidase. *Meth. Enzymol* 1994;244:604–15.
- Abdul Alim M, Tsuji N, Miyoshi T, et al. Characterization of asparaginyl endopeptidase, legumain induced by blood feeding in the ixodid tick *Haemaphysalis longicornis*. *Insect Biochem Mol Biol* 2007;37:911–22.
- Liu C, Sun C, Huang H, et al. Overexpression of legumain in tumors is significant for invasion/metastasis and a candidate enzymatic target for prodrug therapy. *Cancer Res* 2003;63: 2957–64.
- Chen JM, Dando PM, Rawlings ND, et al. Cloning, isolation, and characterization of mammalian legumain, an asparaginyl endopeptidase. *J Biol Chem* 1997;272:8090–8.
- Hara-Nishimura I, Inoue K, Nishimura M. A unique vacuolar processing enzyme responsible for conversion of several proprotein precursors into the mature forms. *FEBS Lett* 1991;294:89–93.
- Davis AH, Nanduri J, Watson DC. Cloning and gene expression of schistosoma mansoni protease. *J Biol Chem* 1987; 262:12851–5.
- Sojka D, Hajdusek O, Dvorak J, et al. Ixodes: an asparaginyl endopeptidase (legumain) in the gut of the hard tick *Ixodes ricinus*. *Int J Parasitol* 2007;37:713–24.
- Delcroix M, Sajid M, Caffrey CR, et al. A multienzyme network functions in intestinal protein digestion by a platyhelminth parasite. *J Biol Chem* 2006;281:39316–29.
- Sajid M, McKerrow JH, Hansell E, et al. Functional expression and characterization of schistosoma mansoni cathepsin b and its trans-activation by an endogenous asparaginyl endopeptidase. *Mol Biochem Parasitol* 2003;131:65–75.
- Kilpatrick AM, Dobson ADM, Levi T, et al. Lyme disease ecology in a changing world: consensus, uncertainty and critical gaps for improving control. *Philos Trans R Soc Lond B Biol Sci* 2017;372.
- Steinmann P, Keiser J, Bos R, et al. Schistosomiasis and water resources development: systematic review, meta-analysis, and estimates of people at risk. *Lancet Infect Dis* 2006; 6:411–25.

41. Kaiser M, Milbradt AG, Siciliano C, et al. Tmc-95a analogues with endocyclic biphenyl ether group as proteasome inhibitors. *Chem Biodivers* 2004;1:161–73.
42. Caffrey CR, Mathieu MA, Gaffney AM, et al. Identification of a cDNA encoding an active asparaginyl endopeptidase of *Schistosoma mansoni* and its expression in *Pichia pastoris*. *FEBS Lett* 2000;466:244–8.
43. Fang B, Boross PI, Tozser J, Weber IT. Structural and kinetic analysis of caspase-3 reveals role for S5 binding site in substrate recognition. *J Mol Biol* 2006;360:654–66.
44. Stennicke HR, Salvesen GS. Biochemical characteristics of caspases-3, -6, -7, and -8. *J Biol Chem* 1997;272:25719–23.
45. Liebschner D, Afonine PV, Baker ML, Bunkoczi G, et al. Macromolecular structure determination using X-rays, neutrons and electrons: recent developments in PHENIX. *Acta Crystallogr D Struct Biol* 2019;75:861–77.
46. Moriarty NW, Grosse-Kunstleve RW, Adams PD. Electronic ligand builder and optimization workbench (elbow): a tool for ligand coordinate and restraint generation. *Acta Crystallogr D Biol Crystallogr* 2009;65:1074–80.
47. Moriarty NW, Draizen EJ, Adams PD. An editor for the generation and customization of geometry restraints. *Acta Crystallogr D Struct Biol* 2017;73:123–30.
48. Afonine PV, Grosse-Kunstleve RW, Echols N, et al. Towards automated crystallographic structure refinement with PHENIX. *Acta Crystallogr D Biol Crystallogr* 2012;68:352–67.
49. Emsley P, Lohkamp B, Scott WG, Cowtan K. Features and development of COOT. *Acta Crystallogr D Biol Crystallogr* 2010;66:486–501.
50. Mathieu MA, Bogyo M, Caffrey CR, et al. Substrate specificity of schistosome versus human legumain determined by p1-p3 peptide libraries. *Mol Biochem Parasitol* 2002;121:99–105.
51. Bogyo M, Shin S, McMaster JS, Ploegh HL. Substrate binding and sequence preference of the proteasome revealed by active-site-directed affinity probes. *Chem Biol* 1998;5:307–20.
52. Kisselev AF, Goldberg AL. Proteasome inhibitors: from research tools to drug candidates. *Chem Biol* 2001;8:739–58.
53. Lee DH, Goldberg AL. Proteasome inhibitors: valuable new tools for cell biologists. *Trends Cell Biol* 1998;8:397–403.
54. Rock KL, Gramm C, Rothstein L, et al. Inhibitors of the proteasome block the degradation of most cell proteins and the generation of peptides presented on MHC class I molecules. *Cell* 1994;78:761–71.
55. Rotonda J, Nicholson DW, Fazil KM, et al. The three-dimensional structure of Apoptain/CPP32, a key mediator of apoptosis. *Nat Struct Biol* 1996;3:619–25.
56. Mittl PR, Di Marco S, Krebs JF, et al. Structure of recombinant human CPP32 in complex with the tetrapeptide acetyl-asp-val-ala-asp fluoromethyl ketone. *J Biol Chem* 1997;272:6539–47.